Transportation Research Part B 190 (2024) 103052

Contents lists available at ScienceDirect

Transportation Research Part B

journal homepage: www.elsevier.com/locate/trb

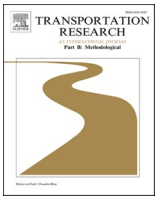

Local detouredness: A new phenomenon for modelling route choice and traffic assignment

Thomas Kjær Rasmussen [a,*], Lawrence Christopher Duncan [a], David Paul Watling [b], Otto Anker Nielsen [a]

[a] Department of Technology, Management and Economics, Technical University of Denmark Akademivej, Bygning 358, 2800 Kgs. Lyngby, Denmark
[b] Institute for Transport Studies, University of Leeds, 36-40 University Road, Leeds, LS2 9JT, United Kingdom

ARTICLE INFO

Keywords:
Local detouredness
Local and global bounds
Route choice model
Stochastic user equilibrium
Consistent choice sets

ABSTRACT

This study introduces the novel concept of local detouredness, i.e. detours on subsections of a route, as a new phenomenon for understanding and modelling route choice. Traditionally, Stochastic User Equilibrium (SUE) traffic assignment models have been concerned with judging the attractiveness of a route by its total route cost. However, through empirical analysis we show that considering solely the global properties of a route is insufficient. We find that it is important to consider local detouredness both when determining realistic and tractable route choice sets and when determining route choice probabilities. For example, analysis of observed route choice data shows that route usage tends to decay with local detouredness, and that there is an apparent limit on the amount of local detouredness seen as acceptable. No existing models can account for this systematically and consistently, which is the motivation for the new route choice model proposed in this paper: the Bounded Choice Model with Local Detour Threshold (BCM-LDT). The BCM-LDT model incorporates the effect of local detouredness on route choice probability, and has an in-built mechanism that assigns zero probabilities to routes violating a bound on total route costs and/or a threshold on local detouredness. Thereby, the model consistently predicts which routes are used and unused. Moreover, the probability expression is closed-form and continuous. SUE conditions for the BCM-LDT are given, and solution existence is proven. Exploiting the special structure of the problem, a novel solution algorithm is proposed where flow averaging is integrated with a modified branch-and-bound method that iteratively column-generates all routes satisfying local and global bounds. Numerical experiments are conducted on small-scale and large-scale networks, establishing that equilibrated solutions can be found and demonstrating the influence of the BCM-LDT parameters on choice set size and flow allocation.

1. Introduction and motivation

Traffic assignment models are widely used to assess transport policies and to predict the impact of future changes in demand. The two most dominant theories of route choice that have underpinned such models are Deterministic User Equilibrium (DUE) (Wardrop, 1952) and Stochastic User Equilibrium (SUE) (Daganzo & Sheffi, 1977), and these have been used in a great many settings, e.g. with

* Corresponding author at: Department of Technology, Management and Economics, Technical University of Denmark Akademivej, Bygning 358, 2800 Kgs. Lyngby, Denmark.
E-mail address: tkra@dtu.dk (T.K. Rasmussen).

https://doi.org/10.1016/j.trb.2024.103052
Received 1 August 2023; Received in revised form 7 June 2024; Accepted 12 August 2024
Available online 13 September 2024

time-dependent travel times/flow as in dynamic models (Han, 2003; Smith, 1993; Smith & Wisten, 1995; Friesz & Han, 2019), with uncertainty in traveller perceptions (Daganzo & Sheffi, 1977; Prashker & Bekhor, 2004; Zhou et al., 2012; Kitthamkesorn & Chen, 2013; Meng et al., 2008; Duncan et al., 2022b), or by presuming bounded rationality in the decision-making (Mahmassani & Chang, 1987; Guo & Liu, 2011; Lou et al., 2010; Di et al., 2013; Di et al., 2016). DUE models assume that a route will be completely unused if it has an even slightly larger cost than the minimum for an OD movement. This is practically unrealistic, both because travellers cannot perceive costs with perfect accuracy and because modellers do not know with certainty the relative influence of the factors that motivate route choice. SUE models relax this assumption by including random disturbances in the perceived travel costs, and through this mechanism spread traffic over a wider range of routes, not just those with minimum cost. In SUE models, the routes actually used are either identified by pre-generating a choice set and then assigning to all such routes (Friedrich et al., 2001; Prato & Bekhor, 2006; Dijkstra, 1959; Sheffi & Powell, 1982; Ben-Akiva et al., 1984; Kitthamkesorn & Chen, 2013), heuristically by terminating an equilibrium algorithm applied to the universal set of acyclic routes after a finite number of iterations (Damberg et al., 1996; Bell et al., 1997; Bazaraa et al., 2013), or by embedding the identification of used routes within the random utility specification and hence the equilibration process (Watling et al., 2015; Watling et al., 2018; Duncan et al., 2022a,2023).

Whichever of the SUE approaches above is adopted, a common feature is that the attractiveness of an alternative is judged by qualities of the complete route, what we shall term *global* properties of the route. These global properties include total length, travel time, travel time (un)reliability, and direct monetary costs such as might be imposed through road pricing. Our contention is that these global properties alone are insufficient for identifying routes that are unattractive and unlikely to be used, and that this severely limits the potential for all existing SUE models to capture realistic route choice behaviour. In the following subsections we provide the basis for this assertion as motivation for the present work, before outlining the challenge addressed by the new method developed in the paper, which for the first time combines *local* with global properties within an SUE framework (in the sense to be explained).

1.1. Empirical motivation

Urban road transport networks are dense and highly complex. Consequently, the set of all possible route alternatives for each traveller in the network is in principle extremely large. Many of these alternatives are however only minor variants on each other, being different only on small subsections where one alternative may detour the other. The same is true for long (national or international) journeys, where a great many very similar route variants exist. One such example is of a main motorway route, for which many slightly different alternatives exist by, rather than staying on the motorway, taking an off-ramp and immediately returning to the motorway on the corresponding on-ramp. Considering a segment of a complete trip where such an alternative exists (a "paired alternative segment" in the language of Bar-Gera (2010)), then the detour may amount to considering a trip segment travel time of (say) 1.5 minutes on the detour compared with 1 minute on the direct route, i.e. a *relative local detour* of 50 % relative to the fastest option. However, on the global level of a complete route, adding half a minute to a journey of, say, two hours is extremely small. The assumed variance in any SUE-based method is almost certain to include such alternatives, of which there will be a great many. However, behaviourally, such alternatives, dependent on the size of the relative local detour, may not be considered by travellers and hence be implausible.

To further demonstrate this point, consider Fig. 1A-B. Fig. 1A displays the results of a GoogleMaps search of routes from Copenhagen to Rome (Google, n.d.), with two reasonable main alternatives generated that are relatively similar in travel time[1]. Fig. 1B displays the results of a 10,000-shortest paths search (based on free-flow travel times) for a European arterial road network model developed in the TransTools project (Jensen et al., 2019). Although somewhat difficult to display, zooming in on Fig. 1B will indeed reveal (highlighted in colours) the 9,999 minor deviations generated as alternatives to the fastest of the two routes generated by the GoogleMaps search. The second main route in Fig. 1A is not captured in Fig. 1B, due to there being such a huge number of combinations of local detours along the fastest main route, even without motorway on-off-ramps being represented in the network. This clearly illustrates the weakness of using K-shortest paths for initial route generation, as in order to capture the other main alternatives, an enormous number of alternatives would need to be generated, many of which would be unrealistic but would attract flow under an SUE model, due to their apparently attractive nature in terms of total route travel time. This phenomenon is in fact more general, not being specific to the K-shortest path approach; for example, using a stochastic shortest path method for pre-generation would replace the need for a large K with the need for a large variance in the random utility model. It would also apply to the SUE methods referenced above that are not based on pre-generation of a choice set, since they are all based on global properties of the complete route, not on the local properties of a route relative to the best alternatives.

That travellers tends to avoid local detours can also be observed from real observed route choice data, as exemplified in Fig. 2. The Fig. illustrates, for a set of 8009 observed route choices collected among car drivers in the Greater Copenhagen Area, the cumulative share of observations as a function of the maximum relative local detour of the observed route[2], as well as a corresponding cumulative curve for the surplus complete route cost relative to the minimum (global detour). As noted previously by several authors (Zhu & Levinson, 2015; Hadjidimitriou et al., 2015; Nielsen, 1996, 2004; Bekhor et al., 2006; Duncan et al., 2022a), at the level of complete route there is strong evidence from actual behaviour that drivers use non-minimum cost routes, that the use of these routes decays with

[1] The longer route deviates from the fastest route along a sub-path that is 6 % longer in travel time than that on the fastest sub-path.

[2] For a given route, we define the maximum relative local detour as the largest detour relative to the shortest sub-route for any trip segment of the route. Travel cost is based on a weighted sum of congested travel time and length, where the weightings have been calibrated according to tracked route observation data (Duncan et al., 2022a). See Prato et al. (2014) for a description of the dataset used.

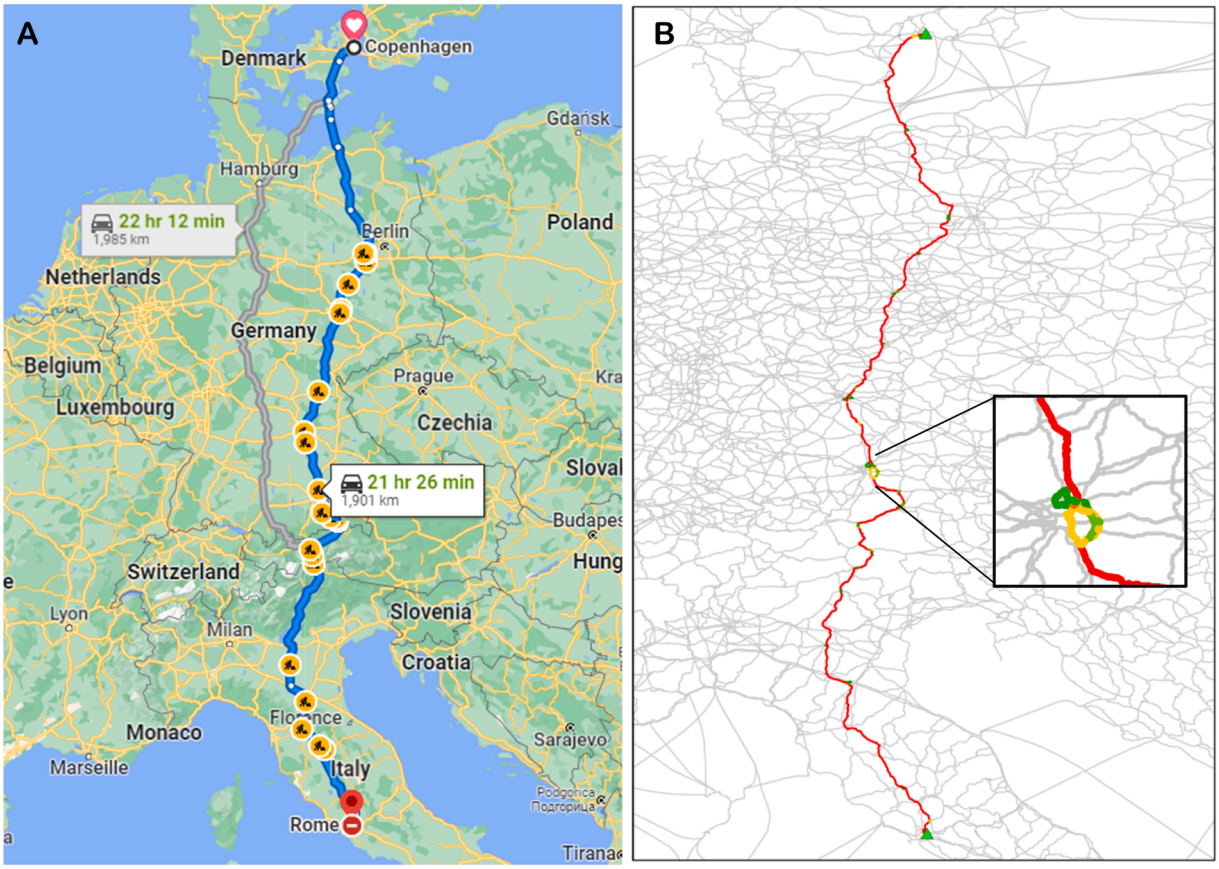

Fig. 1. Routes from Copenhagen to Rome. A: 2 alternative routes generated from a GoogleMaps search. B: 10,000 alternative routes generated from a K-shortest path search in the road network used in the TransTools transport model (Jensen et al., 2019).

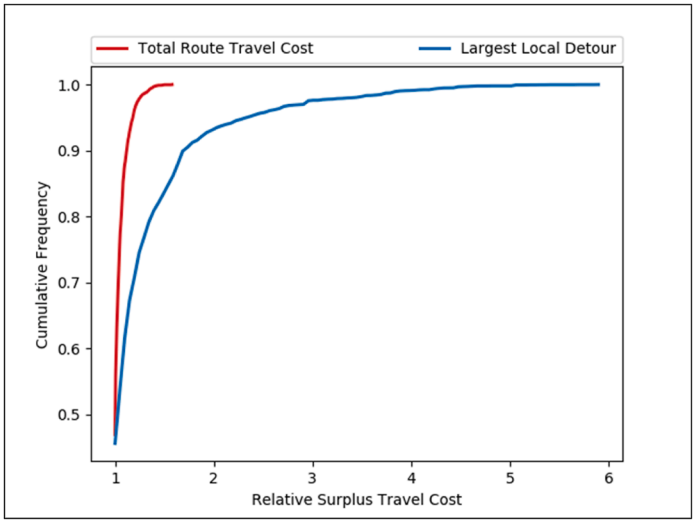

Fig. 2. Distribution of largest local detour among a dataset of 8009 trips collected by GPS in the Greater Copenhagen Area. Largest local detour measured as the largest relative surplus travel cost from the cheapest route for any subsegment of the trip. Distribution of relative surplus total route travel cost also shown.

travel cost, and that there is an apparent limit on the amount of relative surplus total route travel cost drivers are willing to consider. Fig. 2 now adds the insight that a corresponding kind of phenomenon occurs for local, as opposed to global, detours. It can be seen that some travellers – in this case 55 % of them – do use routes containing local detours, but also that there is an upper limit to how large a detour is considered since, for example, 98 % of observed routes have a maximum relative local detour of less than 2.1. Thus, we have evidence that drivers do use some routes including local detours, but route usage decays with an increase in the maximum relative local detour of the route, with an apparent limit again on the amount of "local detouredness" seen as acceptable. This opens up the possibility that local detouredness could be a new additional phenomenon for understanding and modelling route choice, in additional to global travel cost.

While we have argued that local detouredness *could* be an important new attribute, not previously considered in route choice modelling, the argument would be weakened if it is simply a proxy for the global travel cost. It might be believed that *ceteris paribus* a longer route will tend to have both a higher global cost and a higher local detouredness, and so we ask the question: would considering local detouredness likely add anything new? Actually, the argument given around Fig. 1 relating to the K-shortest path example already gives a clue that these global and local factors must be measuring different dimensions of behaviour, otherwise it would not be so problematic to generate the two main alternatives that are clear from Fig. 1A. To add additional weight to this view, Fig. 3 is a scatter plot of relative surplus total route travel cost (global detour) against local detouredness, for the observed data of actual driver route choices as described earlier for Fig. 2. While some used routes are highly efficient in terms of both global cost and local detouredness (bottom left corner of plot), there appears to be little discernible correlation between the two attributes otherwise. A low relative surplus travel cost can have a large local detour, and *vice versa*. Local detouredness thus appears to be a new, distinct attribute for understanding route choice.

1.2. Modelling motivation

As noted earlier, DUE and SUE have been the dominant approaches in modelling traffic network equilibrium for many decades. DUE excludes the possibility of both global detours (only minimum cost routes are used) and local detours (which violate the DUE principle for the trip segment). Thus, DUE assumes all chosen routes are at the point (1,1) in Fig. 3, whereas clearly observed routes in that Fig. cover a much wider range. For SUE models, while the concept of local detours has not previously been considered, there is a concept that might appear to show some passing similarity, namely route *correlation*. That is to say, the similarity between routes is partly explained by route overlap both in the measured travel cost and the unexplained variation. In the following small example, we therefore consider the impact of local detours, and contrast DUE, Multinomial Logit (MNL) SUE (Luce, 1959; Bierlaire, 1998) which neglects route correlation, and Path Size Logit (PSL) SUE (Ben-Akiva & Ramming, 1998; Duncan et al., 2020, 2022b) which corrects for route correlation. In addition, we show the corresponding results for the Bounded Choice Model (BCM) SUE (Watling et al., 2018), which generalises MNL by including a global bound on the surplus total route travel cost considered, to consider how and whether this may also be a mechanism for controlling local detouredness. Finally, previewing the developments set out later in the paper, we give results for a new modelling approach, BCM-LDT SUE, which extends BCM SUE by incorporating separate bounds on local and global detours. Our objective in contrasting these approaches is again to motivate our later work, but this time by illustrating how the consideration of local detours adds a feature to modelling that is not readily captured by existing network modelling approaches.

In the small toy network example in Fig. 4, we consider a problem consisting of two main routes (Routes 2&3) with equal or almost equal travel cost, with an additional route (Route 1) consisting of a large relative local detour to Route 2. To illustrate our point, it is sufficient that the travel costs are constant, not dependent on flow (thus representing a low congestion scenario). The assumed parameter values in the various models are given in the caption of Fig. 4. The two examples and corresponding tables illustrate the sensitivity of choice probabilities when a marginal change of link costs from 201 to 200 on the lower route (Route 3) is made.

Under a Deterministic choice probability scheme (i.e. non-congested DUE), no traveller uses the route with the large local detour (Route 1) in either scenario, but does so at the price of extreme sensitivity of the Route 2&3 route probabilities to the minor change in travel cost on Route 3, with the choice probabilities changing from 0.5&0.5 to 0&1 on these two routes. This is behaviourally very unlikely. In contrast, MNL gives robust results between Routes 2&3 across the two scenarios. However, MNL assigns almost equal probabilities across all three routes (due to the almost-equal global costs), not capturing the behaviourally unrealistic large relative local detour of Route 1. PSL SUE corrects for route overlap, thereby allocating similar total probabilities between (i) the combination of the two highly overlapping routes Routes 1&2 (total share: $0.24+0.25=0.49$ in both scenarios) and (ii) the distinct Route 3 (share: 0.50 and 0.51 in the two scenarios, respectively). However, it can be seen that this is quite a different issue to the existence of local detours: in both scenarios, PSL allocates apparently unrealistic probabilities to the route with the large relative detour (Route 1). Clearly in a large network this may scale up, so traffic may drop unrealistically on motorways between ramps, with unrealistically many travellers taking local detours at the ramps.

Fig. 4 also shows the results from the BCM, which in spite of including a bound on total route cost, is unable to remove significant flow from the local detour route. For the unrealistic Route 1 to be unused in the BCM, one would have to set a very tight bound on relative surplus cost, which would likely leave many attractive routes unused when applied to a larger case. Finally, the BCM-LDT model, which will be explained in detail subsequently in this paper, is a method that includes bounds on both global detour and local detours, and gives what we would suggest is a more plausible allocation of probability between routes in this case, with no use of the local detour route and almost equal use of the two remaining routes with similar travel cost.

Overall, this example gives further support to the hypothesis that local detouredness is a new concept in route choice modelling that cannot be captured by the existing mechanisms and model features available in DUE and SUE approaches. This presents a new challenge, and is very different specifically from our own recent work on the BCM SUE model. This is due to the fact that BCM only

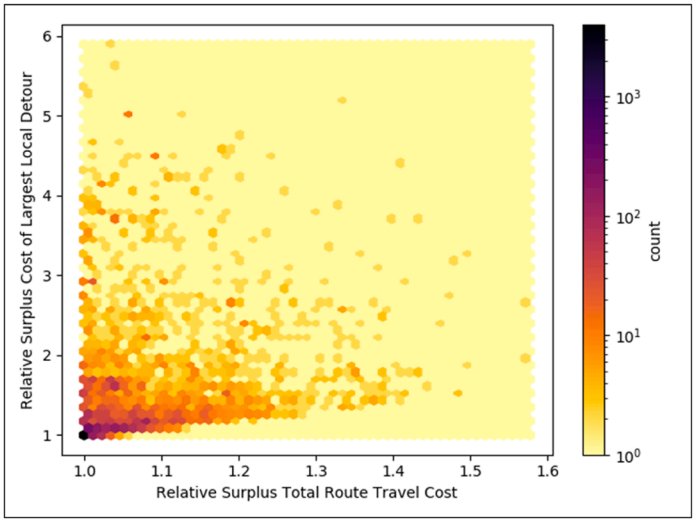

Fig. 3. Plotting relative surplus total route travel cost versus relative surplus cost of largest local detour of route observations in Fig. 2.

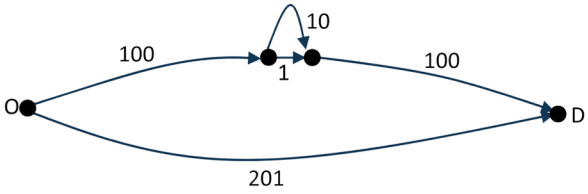

Route	Deterministic	MNL	PSL	BCM	BCM-LDT
1	0.00	0.31	0.24	0.30	0.00
2	0.50	0.34	0.25	0.35	0.50
3	0.50	0.34	0.50	0.35	0.50

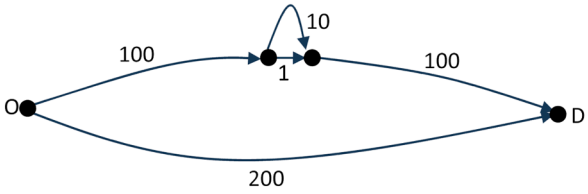

Route	Deterministic	MNL	PSL	BCM	BCM-LDT
1	0.00	0.31	0.24	0.30	0.00
2	0.00	0.34	0.25	0.35	0.49
3	1.00	0.35	0.51	0.35	0.51

Fig. 4. Small uncongested network example, and choice probabilities with Deterministic, MNL, PSL, and BCM models as well as the proposed BCM with Local Detour Threshold (BCM-LDT) model. The number next to each link represents its cost, and demand originates in O and has destination in D. Routes 1-3 are top, middle, and bottom routes, respectively. Logit cost scaling parameter θ_1: 0.01; Path Size scaling parameter β: 1; Relative surplus cost bound parameter τ: 1.5; Local detouredness scaling parameter θ_2: 0.2; Local detour threshold parameter γ: 1. See Section 4.1 for BCM and Section 4.3 for BCM-LDT model/parameter definitions.

applies a bound on the 'global' detour of the full trip. Thus, even with a tight bound on global detour, this in real-life networks will induce many alternatives with high local detours to be used within the model. Fig. 5 illustrates this by considering one OD-movement in the Anaheim network (see Fig. 13), showing the largest relative local detour on routes with a relative route-level cost 1.6 times that of the minimum cost route[3]. This example illustrates that the features seen in the toy network above are phenomena we will expect to see in larger networks, and also highlights the new challenge we are addressing relative to our own previously published work.

1.3. *Specific paper contribution*

In sub-section 1.1 we presented empirical evidence that: (i) local detours may be significant in number and effect in realistic-sized

[3] The network and the particular OD-movement (Origin node: 4, Destination node: 7) shall be introduced later in Section 4.5. The analysis is done with a cost function considering free-flow travel time (measured in minutes, weight 1.0) and distance (measured in kilometres) with a weight of 0.5.

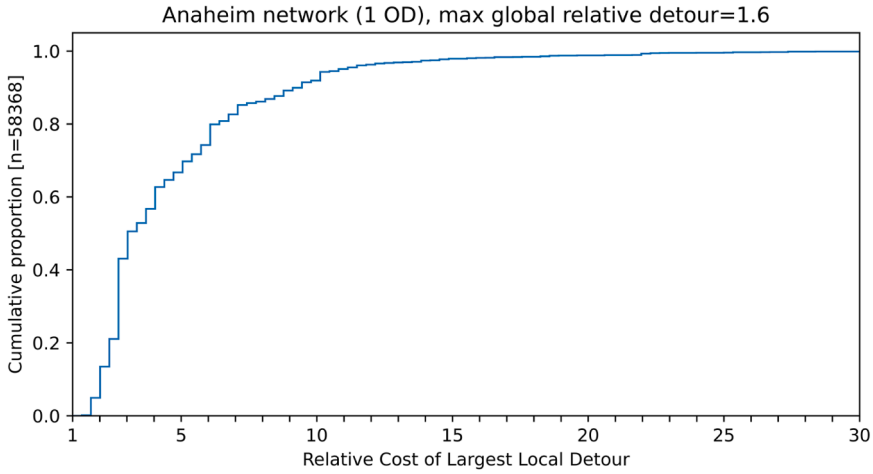

Fig. 5. Distribution of largest local detour among all routes that have relative route-level costs within 1.6 times the minimum cost route (BCM choice set with global bound 1.6), 1 OD-relation on the Anaheim network (Origin node: 4, Destination node:7).

networks; (ii) local detours are not readily accounted for through existing route choice set pre-generation methods; (iii) local detouredness is a new dimension for modelling route choice behaviour that explains some features of observed route choices; and (iv) from observed route choices, the local detouredness of a route is not simply correlated with route cost, it is a distinct route attribute. In sub-section 1.2, we presented modelling evidence demonstrating that the impact of local detours in networks cannot be represented through existing route choice modelling methods, even indirectly; it is a distinctly new modelling challenge.

One approach to addressing these observations could be to argue that new route generation algorithms are needed, that exclude routes with large local detours, thus allowing existing SUE methods to apply to the pre-generated choice set. Indeed, we have experimented with such an approach ourselves, and found it could be effectively implemented. In doing so, we found it to offer a potentially enormous computational advantage in reducing the candidate set of routes from which to choose. However, we believe that such an approach is undesirable for several reasons:

- A strict exclusion criterion must be applied to remove routes. Although we have evidence that routes with large local detours may in some cases be undesirable, this is not equivalent to suggesting that *all* such routes should be excluded. As shown in Fig. 3, some actually chosen routes exist with large local detours. Our argument is not to strictly exclude local detours, but to consider the effect of local detouredness on route choice through some functional/behavioural relationship.
- Intuitively, it makes sense that local detouredness should depend upon generalised travel cost, rather than simply just length, since a detour relatively short in length may be relatively long in terms of generalised travel cost. However, the congested costs are only known in equilibrium, and so the impact of local detouredness should be included within the definition of equilibrium. In doing so, this means that the use of routes with local detours is then dependent upon policy measures (e.g. capacity changes, tolls), and in the case of congested road networks, vehicle flow (through travel time). Doing so ensures that there is consistency between the route generation and route choice probability criteria.
- Most pre-generation methods are not developed from statistical theory and therefore do not readily admit robust estimation methods when data are available. A preferable approach, we contend, is one developed from probabilistic choice theory, which naturally allows standard statistical estimation methods to be in future applied in order to calibrate the model parameters, e.g. controlling the relative influence of local detouredness and global travel cost in terms of the effect on both route availability and route choice probabilities.

By implication, our intention is to address all of the limitations detailed above. We shall develop a behavioural model combining the effects of global route cost and local detouredness of a route. In order to do so, we develop a novel, probabilistic, conjunctive choice model, composed of bounded choice models applied to each of several 'aspects' that influence choice (these terms are specifically defined in Section 3). Importantly, this choice model incorporates both choice set generation and choice of an alternative in one combined approach. When applied in our specific context, where the aspects are travel cost and local detouredness, the model is parameterised such that it is able to reflect both the combined effect of these aspects on route choice probabilities, and the existence of bounds as parameters that reflect the limits observed on these aspects in actual route choices. The full model embeds the behavioural sub-model in an equilibrium framework, so that the set of used routes emerges at equilibrium, based on the equilibrated costs, rather than being pre-generated. In particular by developing the model as a continuous mapping, we prove theoretical existence of equilibria. The whole model is implemented in a solution algorithm that can be applied to general networks.

This is a significant and novel contribution since: a) to our knowledge, local detouredness has never before been considered in choice set generation methods for route choice (which we have shown above to be an important factor to consider), and b) route generation via considering bounds on local detouredness (and total route cost) is implicitly dealt with when solving the proposed route

choice / SUE model. The latter has the positive behavioural implications of being able to generate realistic route choice sets that are consistent with the route choice probability criteria, and, moreover, being able to consistently consider local detouredness as a distinct route attribute in the route choice. There are also considerable practical benefits in that the route generation criteria can generate tractable route choice sets in which all realistic alternatives are captured, and the route choice / SUE model produces continuous probability/flow outputs, including at the boundary where a route transitions from being used to unused. In addition, it overcomes the numerical issues with standard SUE models that require handling large choice sets where a large number of routes may be assigned very small choice probabilities.

The structure of the paper is as follows. Section 2 introduces notation used throughout the paper. Section 3 integrates the BCM within a conjunctive choice model to formulate a conjunctive bounded route choice model. Section 4 then specifies this model to formulate the proposed BCM-LDT model and discusses/illustrates its theoretical properties. Section 5 establishes SUE conditions, proves solution existence, develops a novel solution algorithm, and explores the model's properties/features in numerical experiments on a small-scale network as well as the Anaheim network. Section 6 summarises the work and contains thoughts on future research.

2. Notation

We first introduce the basic common notation adopted in the paper. Consider a network as a directed graph consisting of a set of directed links A, set of nodes B (where each directed link connects two network nodes), and origin-destination (OD) pairs m (m=1, 2, …, M). Define the travel demand for OD-pair m as $d_m \geq 0$, and define R_m as the index set of all[4] simple routes (without cycles) for each OD-pair m. Let $B_{mi} \subseteq B$ be the set of nodes belonging to route $i \in R_m$. N_m is the number of routes in R_m and R is the union of the sets R_m.

Denote the flow on route $i \in R_m$ between OD-pair m as x_{mi} and let $\mathbf{x} = (x_{11}, x_{12}, \ldots, x_{1N_1}, x_{21}, x_{22}, \ldots, x_{21}, x_{22}, x_{2N_2}, \ldots, x_{M1}, x_{M2}, \ldots, x_{MN_M})$ be the N-dimensional flow-vector on the universal choice set across all M OD-pairs, so that the notation x_{mi} refers to element number $i + \sum_{k=1}^{m-1} N_m$ in the N-dimensional vector $\mathbf{x}$. Denote the flow on link a as f_a and let $\mathbf{f} = (f_1, f_2, \ldots, f_a, \ldots, f_{|A|})$ be the $|A|$-dimensional link flow-vector where f_a refers to element number a in $\mathbf{f}$.

The convex set of demand-feasible non-negative route flow solutions G is given by:

$$G = \left\{ \mathbf{x} \in \mathbb{R}_+^N : \sum_{i=1}^{N_m} x_{mi} = d_m, m = 1, 2, \ldots, M \right\}, \tag{1}$$

where $\mathbb{R}_+^N$ denotes the N-dimensional, non-negative Euclidean space.

Next, define μ_{ami} equal to 1 if link a is part of route i for OD-pair m and zero otherwise. Then the convex set of demand-feasible link flows is:

$$F = \left\{ \mathbf{f} \in \mathbb{R}_+^{|A|} : f_a = \sum_{m=1}^{M} \sum_{i=1}^{N_m} \mu_{ami} \cdot x_{mi}, \forall a \in A, \mathbf{x} \in G \right\} \tag{2}$$

In vector/matrix notation, let $\mathbf{x}$ and $\mathbf{f}$ be column vectors, and define $\boldsymbol{\Delta}$ as the $|A| \times N$-dimensional link-route incidence matrix. Then the relationship between link and route flows may be written as $\mathbf{f} = \boldsymbol{\Delta}\mathbf{x}$. Define $\mathbf{t}(\mathbf{f})$ ($\mathbf{t}$: $\mathbf{R}_+^{|A|} \rightarrow \mathbf{R}_+^{|A|}$) as the vector of generalised link travel cost functions. Supposing that the travel cost on route i for OD-pair m is additive in the link travel costs of the utilised links then:

$$c_{mi}(\mathbf{t}(\boldsymbol{\Delta}\boldsymbol{x})) = \sum_{a=1}^{A} \mu_{ami} \cdot t_a(\boldsymbol{\Delta}\boldsymbol{x}) (i \in Rm;\ m = 1, 2, \ldots, M;\ \boldsymbol{x} \in G) \tag{3}$$

Define $\boldsymbol{c}(\boldsymbol{t}(\boldsymbol{\Delta}\mathbf{x}))$ ($\mathbf{c}$: $\mathbf{R}_+^N \rightarrow \mathbf{R}_+^N$) as the vector of generalised route travel cost functions.

Table 1 displays a list of the key notation used in this paper.

3. Conjunctive bounded route choice model

In Section 1 we set out the motivation for the present study, in aiming to represent the impact of local detouredness as a distinct route attribute (alongside route travel cost) in both the availability of a route (whether it is used at all) and the choice of a route (the probability of its use). The aim to consistently combine route generation and route choice led us to consider our own previous work on the bounded choice model (Watling et al., 2018). However, this previous work is limited by the fact that there is assumed to be a single composite measure of utility that determines route availability and route choice. If detouredness and travel cost were combined into a single attribute, this would not allow route exclusion to be driven by either high detouredness *or* high travel cost, as we believe it should be. Therefore, an extension of this previous work is needed so that route choice depends on a *conjunction* of attributes, each of which is separately bounded. This therefore leads us to develop a route choice model based on a combination of existing modelling

[4] We shall suppose that there are no pre-defined restrictions on the set of available routes, other than that they are acyclic, but our methods apply equally if R_m is pre-defined such that other routes are excluded, leading to some smaller Master Choice Set. We have avoided referring to this, so as not to confuse the reader between such pre-defined exclusions from the choice set, and those routes that emerge as unused from the equilibration process.

Table 1
Notation.

Notation	Description
A	Set of network links
B	Set of network nodes
M	Number of OD movements
d_m	Travel demand for OD movement m
R_m	Set of routes for OD m
N_m	Total number of routes for OD m
N	Total number of routes
x_{mi}	Flow on route i of OD m
f_a	Flow on link a
$\mathbf{\Delta}$	Link-route incidence matrix
F	Set of demand-feasible link flows
G	Set of demand-feasible route flows
t_a	Travel cost of link a
c_{mi}	Travel cost on route r of OD m
Q^1_{mi}	Cost-BCM choice probability of route i of OD m
Q^2_{mi}	Detour-BCM choice probability of route i of OD m
P_{mi}	BCM-LDT choice probability of route i of OD m
S_{mi}	Set of segments of route r of OD m
K_{ab}	Set of sub-route segment alternatives between node a and node b
k_{abmi}	Sub-route segment alternative taken by route i of OD m between node a and node b
ω_k	Travel cost of sub-route segment alternative $k \in K_{ab}$
ϕ_{mi}	Local detour measure of route i of OD m
θ_1	Travel cost scaling parameter
θ_2	Local detouredness scaling parameter
τ	Relative surplus total route travel cost bound parameter
γ	Local detour threshold parameter
λ_n	Step size at iteration n of BCM-LDT solution algorithm

approaches: probabilistic conjunctive choice models (Section 3.1) and bounded choice models (Section 3.2), which we integrate into a unified route choice model in Section 3.3. We shall then later in Section 4 specify this unified route choice model in terms of the two route aspects travel cost and detouredness, to formulate the proposed model. To simplify the notation below, we suppress reference to the origin-destination movement, with the proviso that routes are clearly only compared with other routes on the same movement.

3.1. Conjunctive choice model

The probabilistic Conjunctive Choice Model (CCM) has been formulated for application in a variety of choice contexts (Jedidi & Kohli, 2005; Gilbride & Allenby, 2004; Swait, 2001; Shin & Ferguson, 2017; Kohli & Jedidi, 2005). Here we formulate it in the context of route choice. Suppose that there is a set of aspects Y that influence travellers' choice of route (in a similar way to which aspects are defined by Tversky (1972)). Aspect $y \in Y$ could for example be a single route attribute (e.g. travel time) or a combination of route attributes (e.g. linear combination of travel time and length). The CCM route choice principle is that travellers choose a route based on the probability of it having the best aspect value for each aspect, i.e. it being the best in all aspects. Under this principle, the probability of choosing route $i \in R$ is:

$$P_i = \frac{\text{Prob(route } i \text{ is best in all aspects in } Y)}{\sum_{j \in R} \text{Prob(route } j \text{ is best in all aspects in } Y)}. \tag{4}$$

The probability P_i is a conditional probability, conditioning on the fact that routes are compared only when they are best in all aspects. The probability that route i is best in all aspects in Y is:

$$\text{Prob(route } i \text{ is best in all aspects in } Y) = \text{Prob}\left(\bigcap_{y \in Y} (\text{route } i \text{ is best in aspect } y)\right) = \prod_{y \in Y} \text{Prob(route } i \text{ is best in aspect } y), \tag{5}$$

assuming that the component probabilities are statistically independent. Thus, inserting (5) into (4), the probability of choosing route $i \in R$ is:

$$P_i = \frac{\prod_{y \in Y} \text{Prob(route } i \text{ is best in aspect } y)}{\sum_{j \in R} \prod_{y \in Y} \text{Prob(route } i \text{ is best in aspect } y)}. \tag{6}$$

In general choice modelling, the CCM has typically been used as a means of 'screening' alternatives (Jedidi & Kohli, 2005; Gilbride & Allenby, 2004; Shin & Ferguson, 2017; Kohli & Jedidi, 2005). 'Cut-offs' are applied to each aspect y to assign Prob(alternative i is best in aspect y) = 0 if the value for aspect y for alternative i is greater/less than some cut-off value (Swait, 2001). Consequently, if for alternative i Prob(alternative i is best in aspect y) = 0 for any aspect y, then $P_i = 0$ and the alternative is 'screened'. In this application of the CCM, the model could be considered to fall under the category of 'consider-then-choose' choice

models. As described by Shin & Ferguson (2017), a non-compensatory screening rule is employed to narrow the set of alternatives to a 'consideration set', and then a compensatory choice rule is employed to decide between the remaining alternatives in the choice set. This aligns with our ambitions in the current study of developing a route choice model that screens alternatives by imposing individual cut-offs to route aspects (total route cost and detouredness), and then choosing from remaining routes based on their overall attractiveness in the route aspects.

3.2. Bounded choice model

The Bounded Choice Model (BCM) (Watling et al., 2018) route choice principle is that travellers choose a route based on the probability of it having the best utility relative to a reference utility. By setting this reference utility equal to the maximum deterministic utility of all alternatives, the attractiveness of a route depends on the utilities of *all* routes, meaning that the BCM falls within the class of relative random utility theory (Zhang et al., 2004; Zhang, 2013, 2015; Leong & Hensher, 2015).

The BCM is derived as follows. Define V_{r^*} as the reference utility of the reference alternative r^*, which in this case is the maximum utility alternative, i.e. $V_{r^*} = \max(V_l : l \in R)$. Thus, if U_i and V_i are the random and deterministic utilities for route $i \in R$, respectively, the difference in random utility for route $i \in R$ relative to the reference utility for route $i \in R$ is:

$$U_{r^*} - U_i = V_{r^*} + \epsilon_{r^*} - V_i - \epsilon_i = V_{r^*} - V_i + \varepsilon_i = \max(V_l : l \in R) - V_i + \varepsilon_i,$$

where ε_i is the individually and identically distributed random variable error term for route $i \in R$, and ε_i is the difference random variable for route $i \in R$ with the reference alternative. The MNL model can be derived by assuming the ε_i error terms are Gumbel distributed and thus the ε_i difference random error terms assume the logistic distribution. The BCM, however, proposes that the difference random variable error terms ε_i assume a truncated logistic distribution, obtained by left-truncating a logistic distribution with mean 0 and scale θ^{-1} at a lower bound of $-\psi$ for some $\psi \geq 0$. As such, a bound is applied to the difference in utility to the reference utility, so that if a route has a utility below the bound, it receives zero choice probability. This means that routes with utilities below the bound have zero probability of being the best alternative (relative to the reference utility).

Given the above, it follows from the derivation of the BCM in Duncan et al. (2022a, Supplementary Material, Appendix A) that the probability of choosing route $i \in R$ is:

$$Q_i = \text{Prob(route } i \text{ is best in utility relative to reference utility)} = \frac{(\exp(\theta(V_i - \max(V_l : l \in R) + \psi)) - 1)_+}{\sum_{j \in R}(\exp(\theta(V_j - \max(V_l : l \in R) + \psi)) - 1)_+}, \tag{7}$$

where $(\cdot)_+ = \max(0, \cdot)$, $\theta > 0$ is a scaling parameter, and $\psi > 0$ is the bound parameter.

3.3. Conjunctive bounded choice model

We now combine the CCM in (4)-(6) and the BCM in (7) to formulate a Conjunctive Bounded Choice Model (CBCM). The CBCM route choice principle is that travellers choose a route based on the probability of it having, for each aspect, the best aspect utility relative to a reference aspect utility (i.e. relatively best in all aspects in Y). Under this principle, the probability of choosing route $i \in R$ is:

$$P_i = \frac{\text{Prob(route } i \text{ is relatively best in all aspects in } Y)}{\sum_{j \in R}\text{Prob(route } j \text{ is relatively best in all aspects in } Y)}. \tag{8}$$

Similar to the CCM, the probability P_i is a conditional probability, conditioning on the fact that routes are compared only when they are relatively best in all aspects in Y. The probability route i is best in all aspects in Y is:

$$\begin{aligned}\text{Prob(route } i \text{ is relatively best in all aspects in } Y) &= \text{Prob}\left(\bigcap_{y \in Y}(\text{route } i \text{ is relatively best in aspect } y)\right) \\ &= \prod_{y \in Y}\text{Prob(route } i \text{ is relatively best in aspect } y),\end{aligned} \tag{9}$$

assuming that the component probabilities are statistically independent. Thus, inserting (9) into (8), the probability of choosing route $i \in R$ is:

$$P_i = \frac{\prod_{y \in Y}\text{Prob(route } i \text{ is relatively best in aspect } y)}{\sum_{j \in R}\prod_{y \in Y}\text{Prob(route } j \text{ is relatively best in aspect } y)}. \tag{10}$$

Now, to determine Prob(route i is relatively best in aspect y) we follow the same process as was used for the derivation of the BCM, as outlined in Section 3.2, but applied to aspect utilities rather than total utilities. It follows from this that the aspect-y-BCM probability of choosing route i is:

$$Q_i^y = \text{Prob(route } i \text{ is relatively best in aspect } y) = \frac{\left(\exp\left(\theta_y\left(V_i^y - \max\left(V_l^y : l \in R\right) + \psi_y\right)\right) - 1\right)_+}{\sum_{k \in R}\left(\exp\left(\theta_y\left(V_k^y - \max\left(V_l^y : l \in R\right) + \psi_y\right)\right) - 1\right)_+}, \tag{11}$$

where V_i^y is the deterministic utility of route i for aspect y, $\theta_y > 0$ is a scaling parameter for aspect y, and $\psi_y > 0$ is the bound parameter for aspect y.

Inserting (11) into (10) above, the probability of choosing route $i \in R$ is then:

$$P_i = \frac{\prod_{y\in Y}\frac{\left(\exp\left(\theta_y\left(V_i^y-\max\left(V_l^y:l\in R\right)+\psi_y\right)\right)-1\right)_+}{\sum_{k\in R}\left(\exp\left(\theta_y\left(V_k^y-\max\left(V_l^y:l\in R\right)+\psi_y\right)\right)-1\right)_+}}{\sum_{j\in R}\prod_{y\in Y}\frac{\left(\exp\left(\theta_y\left(V_j^y-\max\left(V_l^y:l\in R\right)+\psi_y\right)\right)-1\right)_+}{\sum_{k\in R}\left(\exp\left(\theta_y\left(V_k^y-\max\left(V_l^y:l\in R\right)+\psi_y\right)\right)-1\right)_+}} = \frac{\prod_{y\in Y}\left(\exp\left(\theta_y\left(V_i^y-\max\left(V_l^y:l\in R\right)+\psi_y\right)\right)-1\right)_+}{\sum_{j\in R}\prod_{y\in Y}\left(\exp\left(\theta_y\left(V_j^y-\max\left(V_l^y:l\in R\right)+\psi_y\right)\right)-1\right)_+}. \tag{12}$$

The CBCM thus imposes a bound on each aspect. For each aspect y, a bound is applied to the difference between the aspect utility and the aspect reference utility. Thus, if for any aspect y, a route has an aspect utility below the bound, it receives zero choice probability, and therefore has zero probability of being simultaneously the best alternative in all aspects.

A key attractive feature of the CBCM is that the choice probability function is continuous. As Gilbride & Allenby (2004) note, a major deficiency often experienced by choice models that screen alternatives through imposing cut-offs to aspects, is discontinuity of the choice probabilities. In such existing approaches, alternatives entering and exiting the consideration set as aspect values are varied can typically lead to 'abrupt changes' in the choice probabilities. In contrast, the CBCM choice probabilities are a continuous function of the aspect utilities (due to the continuity of the original BCM), including when the aspect utility of a route crosses from below to above the bound (and *vice versa*).

3.4. Limiting behaviour

Here we demonstrate that as each aspect bound tends to infinity (i.e. as $\psi_y \to \infty$, $\forall y \in Y$) the CBCM collapses into a simple MNL model with a linear utility function of each aspect utility. This is explained as follows. First, under the knowledge that as $\psi_y \to \infty$, $\forall y \in Y$, no route $i \in R$ will have any aspect utility that violates $V_i^y \le \max\left(V_l^y : l \in R\right) - \psi_y$, P_i in (12) can be simplified to:

$$P_i = \frac{\prod_{y\in Y}\left(\exp\left(\theta_y\left(V_i^y-\max\left(V_l^y:l\in R\right)+\psi_y\right)\right)-1\right)}{\sum_{j\in R}\prod_{y\in Y}\left(\exp\left(\theta_y\left(V_j^y-\max\left(V_l^y:l\in R\right)+\psi_y\right)\right)-1\right)}.$$

This expression can be re-arranged as follows:

$$P_i = \frac{\prod_{y\in Y}\left(\exp\left(\theta_y V_i^y\right)\exp\left(\theta_y\left(\psi_y-\max\left(V_l^y:l\in R\right)\right)\right)-1\right)}{\sum_{j\in R}\prod_{y\in Y}\left(\exp\left(\theta_y V_j^y\right)\exp\left(\theta_y\left(\psi_y-\max\left(V_l^y:l\in R\right)\right)\right)-1\right)}.$$

Taking out factors of $\exp\left(\theta_y\left(\psi_y-\max\left(V_l^y:l\in R\right)\right)\right)$ for each $y \in Y$ from both numerator and denominator, which cancel out, the following expression is obtained:

$$P_i = \frac{\prod_{y\in Y}\left(\exp\left(\theta_y V_i^y\right)-\frac{1}{\exp\left(\theta_y\left(\psi_y-\max\left(V_l^y:l\in R\right)\right)\right)}\right)}{\sum_{j\in R}\prod_{y\in Y}\left(\exp\left(\theta_y V_j^y\right)-\frac{1}{\exp\left(\theta_y\left(\psi_y-\max\left(V_l^y:l\in R\right)\right)\right)}\right)}.$$

As $\psi_y \to \infty$, $\forall y \in Y$, we get:

$$P_i = \frac{\prod_{y\in Y}\exp\left(\theta_y V_i^y\right)}{\sum_{j\in R}\prod_{y\in Y}\exp\left(\theta_y V_j^y\right)},$$

which is equivalent to:

$$P_i = \frac{\exp\left(\sum_{y\in Y}\theta_y V_i^y\right)}{\sum_{j\in R}\exp\left(\sum_{y\in Y}\theta_y V_j^y\right)}.$$

Thus, in the specific case of all aspect bounds tending to infinity the CBCM is a fully compensatory route choice model, in the sense that it collapses into a simple MNL model with a linear utility function of each aspect utility. However, in the general case of finite aspect bounds (as considered in the present paper), such a relationship no longer holds since the model can assign zero probabilities based on individual aspects.

4. Bounded choice model with local detour threshold (BCM-LDT)

To formulate the Bounded Choice Model with Local Detour Threshold (BCM-LDT) model we specify the CBCM with the following two aspects: total generalised route travel cost and local detouredness. In Sections 4.1 & 4.2 we establish the aspect-y-BCMs

corresponding to each of the aspects of cost and detouredness, respectively, where in Section 4.2 we propose a measure of local detouredness. In Section 4.3 we consequently formulate the BCM-LDT and discuss its properties. In Sections 4.4 & 4.5 we explore the properties of the model on a small-scale network and the Anaheim network, respectively.

4.1. Cost-BCM

The first aspect $1 \in Y$ we consider within the CBCM is total generalised route travel cost. As such, this corresponds to the specification of the BCM studied thus far in Watling et al. (2018) and Duncan et al. (2022a). This 'cost-BCM' supposes that the deterministic aspect utilities are equal to the negative of the total route travel cost, i.e. $V^1_{mi} = -c_{mi}, \forall i \in R_m$. The reference aspect utility is therefore the negative of the cost of the cheapest route: $V^1_{mr^*} = -\min(c_{ml} : l \in R_m)$. Under this configuration of the aspect-y-BCM in (11) above, the choice probability relation for route $i \in R_m$ is:

$$Q^1_{mi} = \frac{(\exp(-\theta_1(c_{mi} - \min(c_{ml} : l \in R_m) - \psi_1)) - 1)_+}{\sum_{j \in R_m}(\exp(-\theta_1(c_{mj} - \min(c_{ml} : l \in R_m) - \psi_1)) - 1)_+}, \tag{13}$$

where $\theta_1 > 0$ is the travel cost scaling parameter for the cost-BCM, representing sensitivity to travel cost (relative to the bound). Since the cost-BCM imposes a bound on total route travel cost, this cost bound is also referred to as the global [cost] bound. In this case, the bound is an absolute bound on surplus total route travel cost, i.e. a route receives zero probability if it has a cost as great as or greater than ψ_1 *plus* the minimum cost route (ψ_1 cost units away from the minimum).

The cost-BCM can also, however, be stipulated with a relative bound on surplus total route cost, by setting $\psi_1 = (\tau - 1) \cdot \min(c_{ml} : l \in R_m)$, so that:

$$Q^1_{mi} = \frac{(\exp(-\theta_1(c_{mi} - \tau \cdot \min(c_{ml} : l \in R_m))) - 1)_+}{\sum_{j \in R_m}(\exp(-\theta_1(c_{mj} - \tau \cdot \min(c_{ml} : l \in R_m))) - 1)_+}, \tag{14}$$

where $\tau > 1$ is the relative surplus total route travel cost bound parameter. In this case, a route receives zero probability if it has a cost as great as or greater than τ *times* the minimum route cost. Note that, for reasons that will be made clearer later, when comparing the proposed BCM-LDT model to the standard cost-BCM, we utilise the model in (14) with global bound stipulated as a relative bound.

4.2. Detour-BCM

The second aspect $2 \in Y$ we consider within the CBCM is local detouredness. In general, the aspect of local detouredness is a consideration of the extent to which a route detours from shortest subroutes at each of its subsections. We propose here a *measure of local detouredness*. Define the *set of segments* S_{mi} for route $i \in R_m$ as the set of ordered node pairings:

$$S_{mi} = \{(a,b) : a \in B_{mi},\ b \in B_{mi} \text{ and node } a \text{ precedes node } b \text{ when traversing route } i \in R_m\}.$$

Note that S_{mi} includes not just ordered node pairings of adjacent nodes, but all ordered node pairs in the route. The *universal set of segments* for all OD-pairs is then:

$$S = \bigcup_{m=1}^{M} \bigcup_{i \in R_m} S_{mi}.$$

Define the set K_{ab} of *segment alternatives* for segment $(a, b) \in S$ as the index set of all simple sub-routes from node a to node b. Furthermore, define the *used segment alternative* for segment $(a, b) \in S_{mi}$ of route $i \in R_m$ as the element $k_{abmi} \in K_{ab}$ denoting the index of the segment alternative actually used by route $i \in R_m$ from node a to node b.

For a given setting of the generalised link costs $\boldsymbol{t}$, the *measure of local detouredness* ϕ_{mi} for route $i \in R_m$ is defined as:

$$\phi_{mi}(\boldsymbol{t}) = \max\left\{\frac{\omega_{k_{abmi}}(\boldsymbol{t}) - \min(\omega_j(\boldsymbol{t}) : j \in K_{ab})}{\min(\omega_j(\boldsymbol{t}) : j \in K_{ab})} :\ (a,b) \in S_{mi}\right\}, \tag{15}$$

where $\omega_k(\boldsymbol{t})$ is the travel cost of segment alternative $k \in K_{ab}$ for segment $(a, b) \in S_{mi}$ of route $i \in R_m$. ϕ_{mi} identifies the maximum relative detour of a route by comparing—for each of that route's segments—the cost of the used segment alternative with the cost of the minimum cost alternative for that segment. Note that this measure of local detouredness is a *relative* measure, i.e. a detour measure of $\phi_{mi} = y$ corresponds to the worst detouring segment of the route being $(100 \times y)$ % or $y + 1$ times greater than the cost of the minimum cost alternative for that segment.

To demonstrate this measure, consider the simple network illustrated in Fig. 6 with one OD-movement A to E. Route 1 is $A \to B \to C \to D \to E$, Route 2 is $A \to B \to D \to E$, and Route 3 is $A \to D \to E$. We demonstrate how the measure of local detouredness for Route 1 can be calculated as follows. We start by identifying all the segments of the route:

$$S_1 = \{(A,B), (A,C), (A,D), (A,E), (B,C), (B,D), (B,E), (C,D), (C,E), (D,E)\}.$$

For segment (B, D), there are two segment alternatives: segment alternative 1 is $B \to D$ and segment alternative 2 is $B \to C \to D$. The index set of segment alternatives for segment (B, D) is $K_{BD} = \{1, 2\}$, where $k = 1$ in K_{BD} refers to segment alternative $B \to D$ and $k = 2$ in

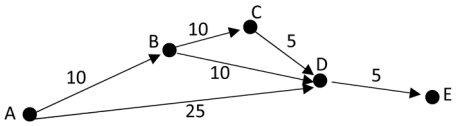

Fig. 6. Example network for demonstrating calculation of local detouredness, with numbers reflecting link travel costs.

K_{BD} refers to segment alternative $B \to C \to D$. The used segment alternative of Route 1 at segment (*B, D*) is $k_{BD1} = 2$. The travel costs of segment alternatives 1&2 are $\omega_1 = 10$ and $\omega_2 = 10 + 5 = 15$. Therefore, the local detouredness of Route 1 at segment (*B, D*) is:

$$\frac{\omega_{k_{BD1}} - \min(\omega_j : j \in K_{BD})}{\min(\omega_j : j \in K_{BD})} = \frac{\omega_2 - \min(\omega_1, \omega_2)}{\min(\omega_1, \omega_2)} = \frac{15 - \min(10, 15)}{\min(10, 15)} = \frac{15 - 10}{10} = 0.5.$$

For segment (*A, D*), the segment alternatives 1-3 are $A \to D$, $A \to B \to D$, and $A \to B \to C \to D$, respectively, with costs 25, 20, & 25. Given Route 1 uses segment alternative 3, the local detouredness of Route 1 at (*A, D*) is $\frac{25-\min(25,20,25)}{\min(25,20,25)} = \frac{5}{20} = 0.25$. For completeness, the local detouredness of Route 1 at segments (*A, E*) and (*B, E*) are $\frac{30-25}{25} = 0.2$ and $\frac{20-15}{15} = 0.33$, respectively, and the rest are equal to 0 due to there being only one segment alternative. The maximum local detouredness of Route 1 from each of its segments in S_1 is thus:

$$\max(0, 0, 0.25, 0.2, 0, 0.5, 0.33, 0, 0, 0) = 0.5,$$

and therefore the measure of local detouredness for Route 1 is $\phi_1 = 0.5$.

For Route 3, the largest detouring segment is (*A, D*) which has local detouredness of $\frac{25-20}{20} = 0.25$, and thus the measure of local detouredness for Route 3 is $\phi_3 = 0.25$. For Route 2, all the used segment alternatives for each of its segments are the minimum costing, and therefore the measure of local detouredness is $\phi_2 = 0$. Thus, while Routes 1&3 have the same total travel cost (=30) and therefore have the same global detour, they have different measures of local detouredness, i.e. detour locally in different ways, where Route 1 is the most locally detouring.

Note that although here to calculate the measure of local detouredness we have for pedagogical purposes enumerated all route segments and all segment alternatives for each segment, it is not necessary to do this in practice. All one needs to know is, for the most detouring segment, the cost of the cheapest segment alternative and the cost of the chosen segment alternative of the route. There are numerous ways this can be done efficiently, and in Section 5.2, we propose a method that indeed avoids the need to enumerate all segment alternatives.

Note that there are alternative measures of local detouredness that one might consider, such as using the average of the relative detours or the sum of the relative detours. The BCM-LDT model to be derived in the following sections can accommodate such alternatives measures, however in this paper we focus on the largest local detour measure, as defined above.

Given the above proposed measure of local detouredness, we formulate the 'detour-BCM', which supposes that the deterministic aspect utilities relate negatively according to local detouredness, i.e. $V^2_{mi} = -\phi_{mi}, \forall i \in R_m$. The reference aspect utility is therefore the minimum detouredness from all routes, which is always equal zero from the minimum cost route: $V^2_{mr^*} = -\min(\phi_{ml} : l \in R_m) = 0$. Under this configuration of the general aspect-*y*-BCM in (11), the choice probability relation for route $i \in R_m$ is:

$$Q^2_{mi} = \frac{(\exp(-\theta_2(\phi_{mi} - \psi_2)) - 1)_+}{\sum_{j \in R_m}(\exp(-\theta_2(\phi_{mj} - \psi_2)) - 1)_+}, \tag{16}$$

where $\theta_2 > 0$ is the detouredness scaling parameter for the detour-BCM, representing sensitivity to local detouredness (relative to the bound). We set the local detour bound to $\psi_2 = \gamma$, where $\gamma > 0$ is the local detour bound parameter.

4.3. Proposed BCM-LDT model

As discussed above, the BCM-LDT model is formulated by specifying the CBCM in (12) with two aspects: total route travel cost and local detouredness. The aspect-1-BCM, the cost-BCM, is as in (14) and the aspect-2-BCM, the detour-BCM, is as in (16). Thus, combining these within the CBCM, the BCM-LDT choice probability relation for route $i \in R_m$ of OD-pair *m*, for a given setting of the (flow-dependent) link costs $\boldsymbol{t}$, is:

$$P_{mi}(\boldsymbol{t}) = \frac{(\exp(-\theta_1(c_{mi}(\boldsymbol{t}) - \tau \cdot \min\{c_{ml}(\boldsymbol{t}) : l \in R_m\})) - 1)_+ (\exp(-\theta_2(\phi_{mi}(\boldsymbol{t}) - \gamma)) - 1)_+}{\sum_{j \in R_m}(\exp(-\theta_1(c_{mj}(\boldsymbol{t}) - \tau \cdot \min\{c_{ml}(\boldsymbol{t}) : l \in R_m\})) - 1)_+ (\exp(-\theta_2(\phi_{mj}(\boldsymbol{t}) - \gamma)) - 1)_+} \tag{17}$$

The BCM-LDT has four standard parameters: $\theta_1 > 0$ is the travel cost scaling parameter (scaling sensitivity to total route cost), $\theta_2 > 0$ is the local detouredness scaling parameter (scaling sensitivity to local detouredness), $\tau > 1$ is the relative surplus total route cost bound parameter, and $\gamma > 0$ is the local detour bound parameter.

Note that as θ_1 multiplies cost and θ_2 multiplies a dimensionless variable (detouredness), then in order to scale the argument of the exponential functions to common units of utility, these parameters will have different units. As a result, θ_1 and θ_2 will have different interpretations, and so may take different values. In Section 5.3.2.4 we explore the impact of the relative values of these two parameters.

The BCM-LDT is continuous in cost and local detouredness under standard assumptions, as shall be proven in Section 5.1. Note that since the BCM-LDT model has two BCM components and thereby two independent bounds on travel cost and local detouredness, in order to distinguish clearly between the two bounds, we refer to the cost-BCM bound on total route cost as the global cost bound, and the detour-BCM bound on local detouredness as a local detour *threshold*. The cost-BCM component assigns a route zero probability if it has a total route cost as great as or greater than τ times the minimum total route cost for that OD-pair. And, the detour-BCM component assigns a route zero probability if, at its most detouring segment, the used segment alternative has a travel cost as great as or greater than $\gamma + 1$ times the minimum costing segment alternative for that segment. A global bound parameter of τ is thus analogous with a local detour threshold parameter of $\gamma + 1$.

We would therefore expect $\tau < (\gamma + 1)$. This is because the detour-BCM component also applies to route-level global detours, and hence **the global cost bound will not influence route exclusion if the local detour threshold is below the cost bound (minus 1)**, though it will influence the choice probabilities. Furthermore, we would not expect to calibrate $\tau > (\gamma + 1)$ from data, since by definition the detouredness is always greater than or equal to the global detour (global detour is also considered in the max-operator of the detouredness measure).

Regarding calibration of the local detour threshold, the derivation of the model from probability theory combined with the continuity property of the model (see Lemma 1 in Section 5.1) allows the threshold to be estimated by rigorous statistical methods, from fitting the model to real-life tracked route observations. For example, this may be achieved in a similar way to how the global cost bound is fitted for the cost-BCM in Duncan et al. (2022a). We discuss this issue in the conclusions section as future research.

We present now the limiting behaviour properties of the BCM-LDT model, noting which models the BCM-LDT model approaches in its limits. These limiting models are (i) the cost-BCM in (14), (ii) a standard MNL in terms of cost, and (iii) an MNL relating linearly to both cost and detouredness, which we show in turn below.

The BCM-LDT model in (17) approaches the cost-BCM in (14) as $\theta_2 \to 0$ and $\gamma \to \infty$ under the condition that γ tends to ∞ faster than θ_2 tends to 0, such that $\lim_{\substack{\theta_2 \to 0 \\ \gamma \to \infty}} \theta_2 \gamma = \infty$. This is explained as follows. It is clear from (17) that the BCM-LDT model is equivalent to the standard cost-BCM in (14) when $(\exp(-\theta_2(\phi_{mi} - \gamma)) - 1)_+$ is equal for all routes $i \in R$ and thus cancels out. If $\gamma \to \infty$, then no route can have a detouredness measure above the threshold and thus in this case $(\exp(-\theta_2(\phi_{mi} - \gamma)) - 1)_+ = \exp(-\theta_2(\phi_{mi} - \gamma)) - 1, \forall i \in R_m$. Now, this expression can be rearranged as follows:

$$\exp(-\theta_2(\phi_{mi} - \gamma)) - 1 = \exp(-\theta_2\phi_{mi})\exp(\theta_2\gamma) - 1 = \exp(-\theta_2\phi_{mi})\exp(\theta_2\gamma) - \frac{\exp(\theta_2\gamma)}{\exp(\theta_2\gamma)}.$$

A factor of $\exp(\theta_2\gamma)$ can be extracted, which will be cancelled out by all routes in the probability relation, leaving $\exp(-\theta_2\phi_{mi}) - \frac{1}{\exp(\theta_2\gamma)}, \forall i \in R_m$. This tends to 1 for all routes as $\theta_2 \to 0$ and $\gamma \to \infty$ under the condition that ψ_2 tends to ∞ faster than θ_2 tends to 0 such that $\lim_{\substack{\theta_2 \to 0 \\ \gamma \to \infty}} \theta_2 \gamma = \infty$.

Note also that since the cost-BCM approaches an MNL model as $\tau \to \infty$ (see Watling et al. (2018)), the BCM-LDT model can also approximate a standard MNL in terms of total route cost. Moreover, following the limiting behaviour of the CBCM demonstrated in Section 3.4, in the limits as both $\tau \to \infty$ and $\gamma \to \infty$, the BCM-LDT model in (17) approaches an MNL model with utility function relating to a linear combination of cost and detouredness, i.e. $V_{mi} = -\theta_1 c_{mi} - \theta_2 \phi_{mi}$ for each route $i \in R_m$. The above properties show that the BCM-LDT is very flexible, as it can collapse to several different models.

The BCM-LDT is multi-objective and thus falls under the category of multi-criteria traffic assignment. Although there are some apparent similarities between the BCM-LDT model and existing bi/multi-criteria models, such as the probability relation used for the Non-Compensatory Stochastic User Equilibrium (NCSUE) model in Ehrgott et al. (2015), the key distinction is that we propose a *conjunctive* as opposed to *disjunctive* choice modelling approach (in the sense described in Cazor et al., 2024). Specifically, the BCM-LDT is based on the probability that an alternative is best in *all* aspects (relative to the corresponding reference aspect values), while the NCSUE probability relation is based on the probability an alternative is best in *at least one* aspect. This is an important distinction, as our contention is that routes should be attractive on the basis of *both* aspects total cost and local detouredness, and so are excluded if unattractive in either.

4.4. Small-scale illustrative example

In this section we illustrate the model proposed above on a small-scale example network. Consider the 4-link network shown in

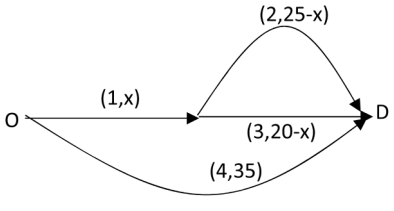

Fig. 7. Small-scale network: 4 link network with 3 routes from origin O to destination D. Notation (A,B) denotes link A with cost B.

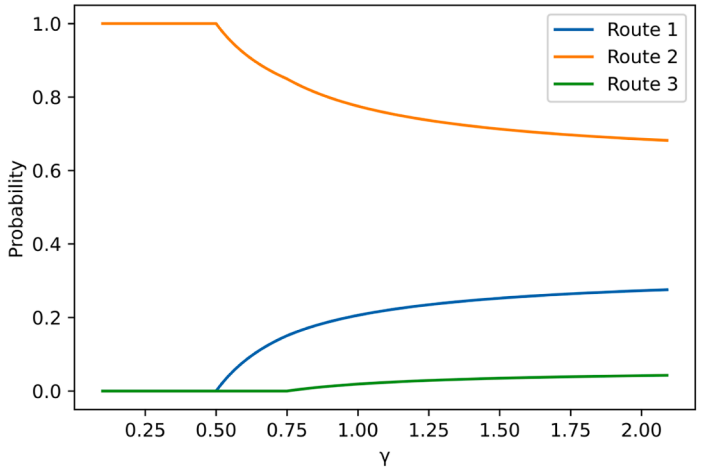

Fig. 8. Small-scale network: BCM-LDT choice probabilities for varying values of γ, assuming $\boldsymbol{\tau} = 2$, $\boldsymbol{\theta}_1 = \boldsymbol{\theta}_2 = 0.1$, and x=10.

Fig. 7. Let x range between 0 and 20, and define Route 1 as consisting of links 1 and 2 with a total cost of 25, Route 2 as the cheapest consisting of links 1 and 3 with a total cost of 20 and Route 3 as consisting of link 4 with a cost of 35. The detouredness measures for Routes 1, 2,and 3 are (25-x-(20-x))/(20-x), 0 and 0.75, respectively. Note that the detouredness measure for Route 3 corresponds to the detour on the (global) route level also. Let $\theta_1 = \theta_2 = 0.1$.

Fig. 8 displays the BCM-LDT choice probabilities of each route as the local detour threshold parameter γ is varied, setting $x = 10$. For x=10, the detouredness measures for Routes 1 and 3 are 0.5 and 0.75 respectively. Consequently, for a local detour threshold less than or equal to 0.5 ($\gamma \leq 0.5$), only Route 2 is used (and thus assigned probability 1). As the threshold increases above 0.5, Route 1 is 'activated' and assigned a non-zero probability that is increasing for increasing threshold values. When the threshold increases above 0.75, Route 3 is also 'activated' and assigned a non-zero probability. The probabilities of Routes 1 and 3 are increasing for increasing threshold values, and in this case as it approaches infinity, the probability share on Routes 1, 2 and 3 approaches the corresponding BCM probabilities (0.331, 0.607 and 0.062, respectively). Also note that, as shown in Section 4.3, as the local detour threshold and global cost bound both tend to infinity ($\gamma \to \infty$ and $\tau \to \infty$), the BCM-LDT approaches MNL choice probabilities based on a linear combination of total route travel cost and detouredness (i.e. utility), where (P_1,P_2,P_3)= (0.331, 0.547,0.122), as expected.

We now turn to analysing the effects of varying both the (relative) local detour threshold and the (relative) global cost bound. Fig. 9 illustrates the flow shares when τ is varied from 1 to 3 and γ from 0 to 3, with all other parameters fixed at their values previously defined above. Route 2 is assigned largest probability, and then Route 1 and Route 3 are introduced (in that order) as the cost bound / detour threshold are loosened (as also found in the case when only the local detour threshold is varied). Route 2 is the minimum cost route and consequently does not have any detours, i.e. this route is always assigned a non-zero choice probability. For low values of the cost bound and detour threshold ($\gamma < 0.5$ and/or $\tau \leq 1.25$), Route 2 is the only used route.

Now, consider a fixed global cost bound and local detour threshold ($\gamma = 1.0$ and $\tau = 2.0$), and let x vary from 0 to 20. Fig. 10 displays the BCM-LDT route choice probabilities. Note that the local and global detour remains constant for Route 3, independent of x. The probability of Route 1 reduces to zero as x increases. This is because the local detour of the route increases as x increases, forcing the probabilities towards zero. At x=15 the detouredness measure of Route 1 is at the threshold $\gamma = 1.0$, and so the model assigns zero choice probability to the route for $x \geq 15$.

Importantly, note the continuity of the probabilities for all experiments, both when varying x and when varying the cost bound and detour threshold values. This is a key feature of the BCM-LDT model that is not trivial to achieve when assigning some routes zero probability.

As demonstrated in Section 1.2, the BCM-LDT model is a very different model to correlation-based models, such as Path Size Logit (PSL) (Ben-Akiva & Ramming, 1998; Duncan et al., 2020), nested GEV-structure models (Vovsha, 1997; Bekhor & Prashker, 1999) and Probit (Daganzo & Sheffi, 1977). These models consider route overlapping from a correlation perspective, whereas our proposed model considers route overlapping from a local detour perspective. While both sets of models take into account route overlapping, their purposes are very different.

To reinforce this point, we compare route choice probabilities from the BCM-LDT model in Fig. 10 with those from the PSL model (see Fig. 11), with Logit scaling parameter equal to 0.1 and path size scaling parameter equal to 1 (see Duncan et al. (2020) for model formulation). Note that the route costs are not equal in this example. At x=0, Routes 1&2 are non-overlapping, i.e. completely distinct routes. As x increases, Routes 1&2 become more overlapping, and at x=20 Route 2 is completely indistinct (all of its route overlaps with Route 1). PSL penalises routes for overlapping (to capture correlation) and therefore as shown in Fig. 11, Route 2's probability decreases as x increases. Route 1 is never completely indistinct as at x=20 it deviates 5 cost units from that of Route 2. Route 1 thus is not penalised as much as Route 2 for overlapping and its choice probability remains relatively constant. Route 3 increases probability as x increases as it gains probability from Route 2. These results are clearly very different to those in Fig. 10.

Note contrastingly that if one were to consider the small-scale network in Fig. 7, with link costs of x, 1-x, 1-x, & 1 for links 1-4,

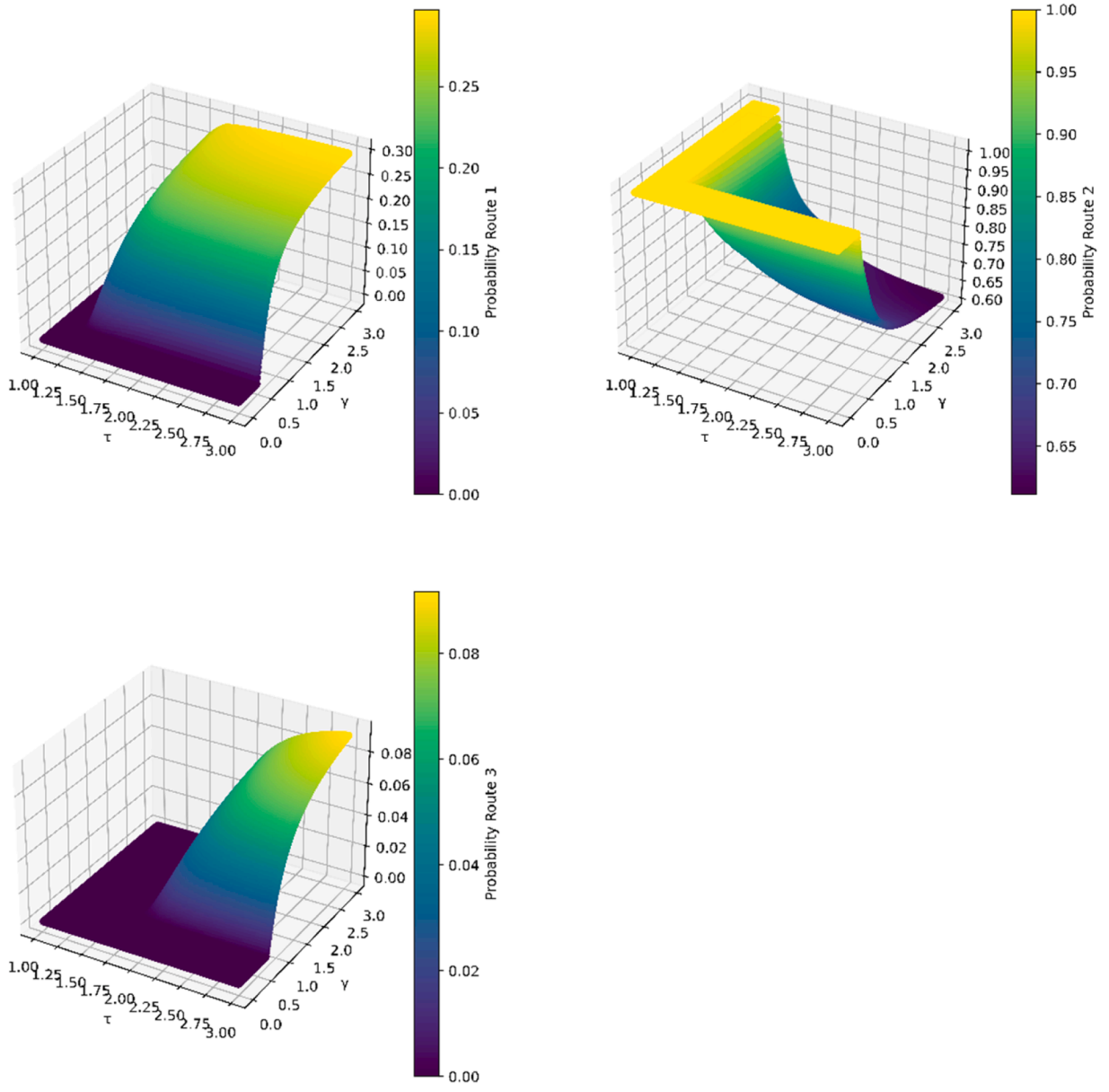

Fig. 9. Small-scale network: BCM-LDT choice probabilities for varying values of γ and τ, each subFig. illustrating the surface for one route, assuming $\boldsymbol{\theta}_1 = \boldsymbol{\theta}_2 = 0.1$, and x=10.

respectively, i.e. the traditional loop-hole network used by Cascetta et al. (1996) to demonstrate route correlation, the BCM-LDT choice probabilities would remain constant at 1/3 as x is varied between 0 and 1. This is because regardless of x the route costs are all equal and there are no local detours (the segment alternatives all have equal costs). The BCM-LDT thereby does not capture route correlation. In Section 6.2 we discuss though the possibilities for extending the BCM-LDT to account for both detouredness and correlation.

Lastly, we explore to what degree each part of Q^1_{mi} and Q^2_{mi} contribute to overall BCM-LDT probability P_{mi} in (17). Q^1_{mi} is the cost-BCM (with a relative bound) in (14) and Q^2_{mi} is the detour-BCM in (16) with $\psi_2 = \gamma$. Fig. 12 displays the probabilities of Q^1_{mi}, Q^2_{mi}, and P_{mi} for each of the three routes in Fig. 7 as x varies between 0 and 20. The first thing to notice is that the Q^1_{mi} cost-BCM choice probabilities are constant since in this example the costs remain constant as x varies. The P_{mi} BCM-LDT probabilities are thus effectively scaled versions of the Q^2_{mi} detour-BCM probabilities, with a constant scaling. As also shown in Fig. 12, the P_{mi} BCM-LDT probability of Route 1 tends to zero as x approaches 15 from below, at which point its local detour first violates the detour threshold. As can be seen with the Q^2_{mi} detour-BCM probability of Route 1, this feature also occurs, except the probability of the route before x=15 is not weighted by its cost-BCM probability.

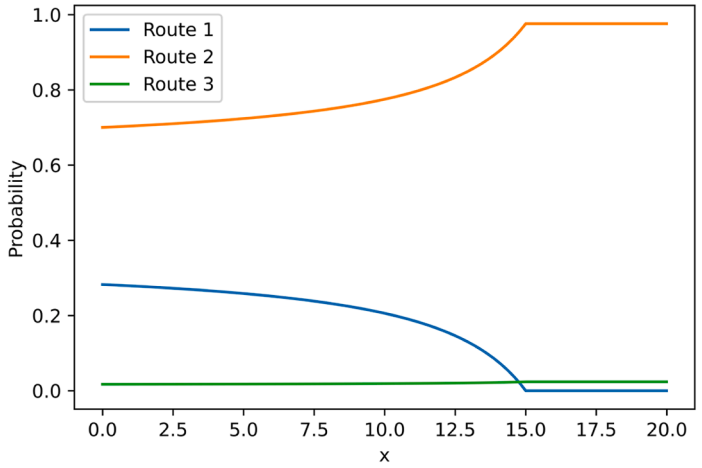

Fig. 10. Small-scale network: BCM-LDT choice probabilities for varying values of x, assuming $\gamma = 1$, $\tau = 2$, $\theta_1 = \theta_2 = 0.1$.

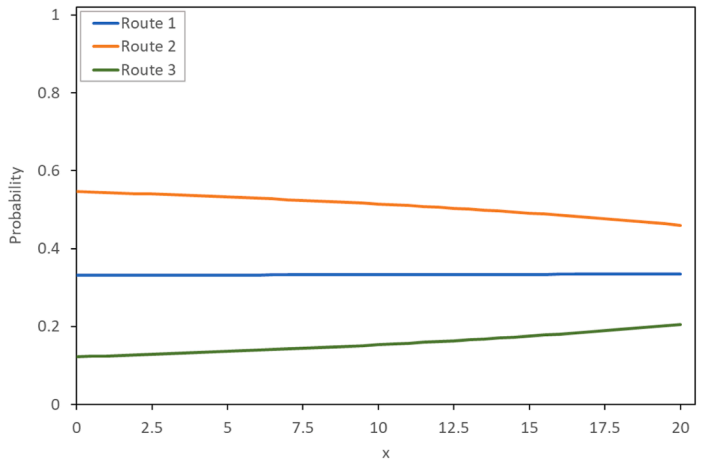

Fig. 11. Small-scale network: Path Size Logit choice probabilities for varying values of x, assuming Logit scaling parameter equal to 0.1 and path size scaling parameter to 1 (See Duncan et al. (2020) for model definition).

4.5. Anaheim network example

In this section we explore and illustrate the effect of γ on both the composition and size of the choice set in a larger-scale network, namely the Anaheim network which is well-known in the transport research community [5]. The network is illustrated in Fig. 13, where blue nodes are network nodes and green nodes are Origin-Destination nodes where links connecting to these can only be used by trips with an origin or destination in these zones. There are 1406 OD-movements with a total demand of 104694.4 trips. In this section, to demonstrate the properties of the BCM-LDT route choice model where the link costs are fixed (flow-independent) and thereby the choice behaviour for each OD is independent, we focus on one OD-relation in the network, namely Origin node 4 and Destination node 7 (marked red in Fig. 13). This corresponds to entering the area on the motorway in the south-east and leaving the area on the same motorway in the north-west. We assume the link generalised cost is a weighted sum of the travel time (in minutes)[6] and length (in kilometers), with weights 1.0 and 0.5, respectively. Note that although in this section we assume fixed link costs and independent OD movements, we shall later apply the BCM-LDT model to SUE where the link costs are flow-dependent and not fixed, and thereby the ODs interact with each other (section 5.3.2).

The set of alternatives that attract flow is heavily dependent on both the local detour threshold and global cost bound. Fig. 14 illustrates the choice set size as function of γ for different values of τ. Note that when $\gamma < \tau - 1$, the choice set of 'active' routes assigned non-zero probability is determined solely by the local detour threshold.

[5] Downloaded from https://github.com/bstabler/TransportationNetworks.
[6] In this experiment we use congested link travel times stemming from a converged User Equilibrium solution provided on the github.

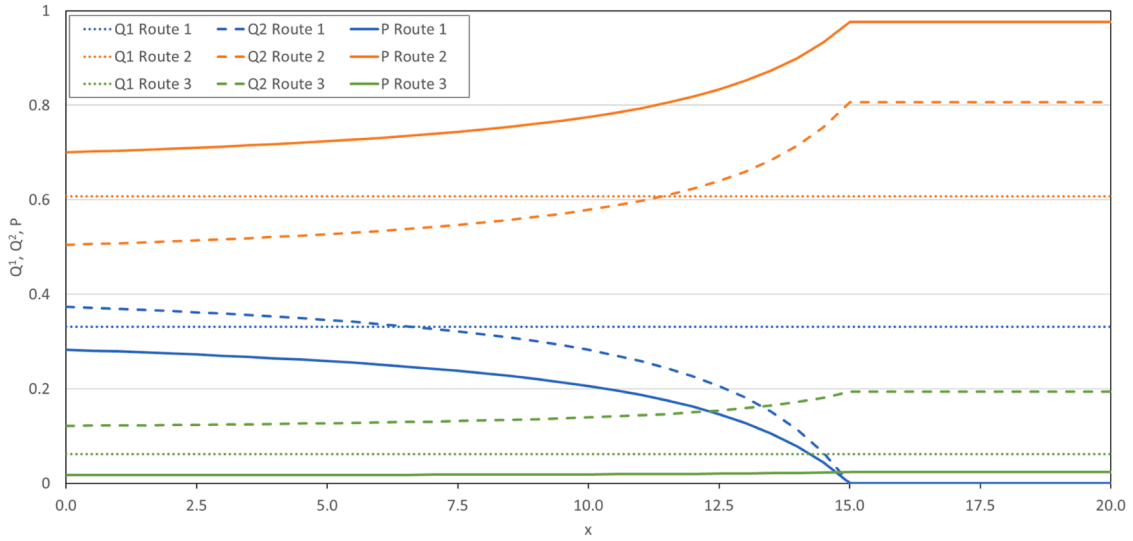

Fig. 12. Small-scale network: Q1 cost-BCM, Q2 detour-BCM, and overall P BCM-LDT choice probabilities for varying values of x, assuming $\gamma = 1$, $\tau = 2$, $\theta_1 = \theta_2 = 0.1$.

The Fig. illustrates the effects of having both a global cost bound and local detour threshold. For $\gamma \leq 0.6$ the choice sets are identical across τ, as mentioned above. As γ is increased beyond 0.6, the (global) cost bound has an effect. If no global cost bound is applied (approximated here with $\tau = 15$) the choice sets become enormously large (e.g. 2,588,503 alternatives when $\gamma = 2.3$), whereas the global cost bound of $\tau = 1.6$ determines an upper size of the choice set of 66,714 routes. For moderate sizes of γ, the set of used routes is largely determined by the local detour threshold. For instance, when $\gamma = 0.8$, approximately 600 routes are generated for all tested values of τ. Choice set sizes of that order of magnitude are much more computationally tractable than if only a global bound of e.g. $\tau = 1.6$ or no bounds at all are applied. Note also that the choice sets are identical in this range of γ when $\tau = 4.0$ and $\tau = 15$, since the choice sets are determined solely by the local detour threshold when $\tau \geq \gamma + 1$ (i.e. choice sets are in this case guaranteed to be identical when $\gamma \leq 3.0$).

Fig. 15 shows the links used by the BCM-LDT for different values of γ when assuming $\tau = 1.6$. For reference, the link usage for the BCM with $\tau = 1.6$ is also included. The widths of the links indicate the link probabilities. As can be seen, the choice set size and number of links used both increase with γ. When $\gamma = 0.1$, there is only one route that is used: the minimum cost route. At $\gamma = 0.4$ there are 6 routes and one can see that there is some variation in the choice set, with routes that differ considerably from the minimum cost route. The choice set size increases rapidly as γ is increased. Note the large choice set size for the BCM ($\gamma = \infty$) case, again highlighting the computational benefit of imposing a threshold on local detours as is done in BCM-LDT for $\gamma < \infty$.

5. Stochastic user equilibrium with the BCM-LDT

In this section, we establish Stochastic User Equilibrium (SUE) conditions for the BCM-LDT, to consistently account for congestion in the network. We then prove solution existence, develop a solution algorithm, and illustrate the methodology with some numerical experiments.

5.1. Equilibrium conditions and solution existence

SUE conditions for the BCM-LDT are as follows:

BCM-LDT SUE: A route flow vector $\boldsymbol{x}^* \in G$ is a BCM-LDT SUE solution iff it is a solution to the fixed-point problem

$$\boldsymbol{x} = \boldsymbol{DP}(\boldsymbol{t}(\boldsymbol{\Delta x})),$$

where P_{mr} is given by (17) for route $r \in R_m$ and $\boldsymbol{D}$ is a $N \times N$ diagonal matrix of the travel demands for each OD-pair (i.e. with d_m on each of the diagonal elements for the route rows/columns belonging to each OD-pair).

We now proceed to prove that BCM-LDT SUE solutions are guaranteed to exist. First, let $H_{mi}(\boldsymbol{x}) = d_m P_{mi}(\boldsymbol{t}(\boldsymbol{\Delta x}))$ be a component of the BCM-LDT SUE mapping, where P_{mi} is the BCM-LDT choice probability function for route $i \in R_m$ given by (17), dependent upon the link cost functions $\boldsymbol{t}(.)$, which are in turn dependent upon the route flows $\boldsymbol{x}$. Let $\boldsymbol{H}(\boldsymbol{x})$ be the vector of functions with components $H_{mi}(\boldsymbol{x})$.

In Lemma 1 we now establish the continuity property of $\boldsymbol{H}(.)$.

Lemma 1. If the link cost function $\boldsymbol{t}(\boldsymbol{\Delta x})$ is a continuous function for all $\boldsymbol{x} \in G$, then $\boldsymbol{H}(\boldsymbol{x})$ is also a continuous function for all $\boldsymbol{x} \in G$.

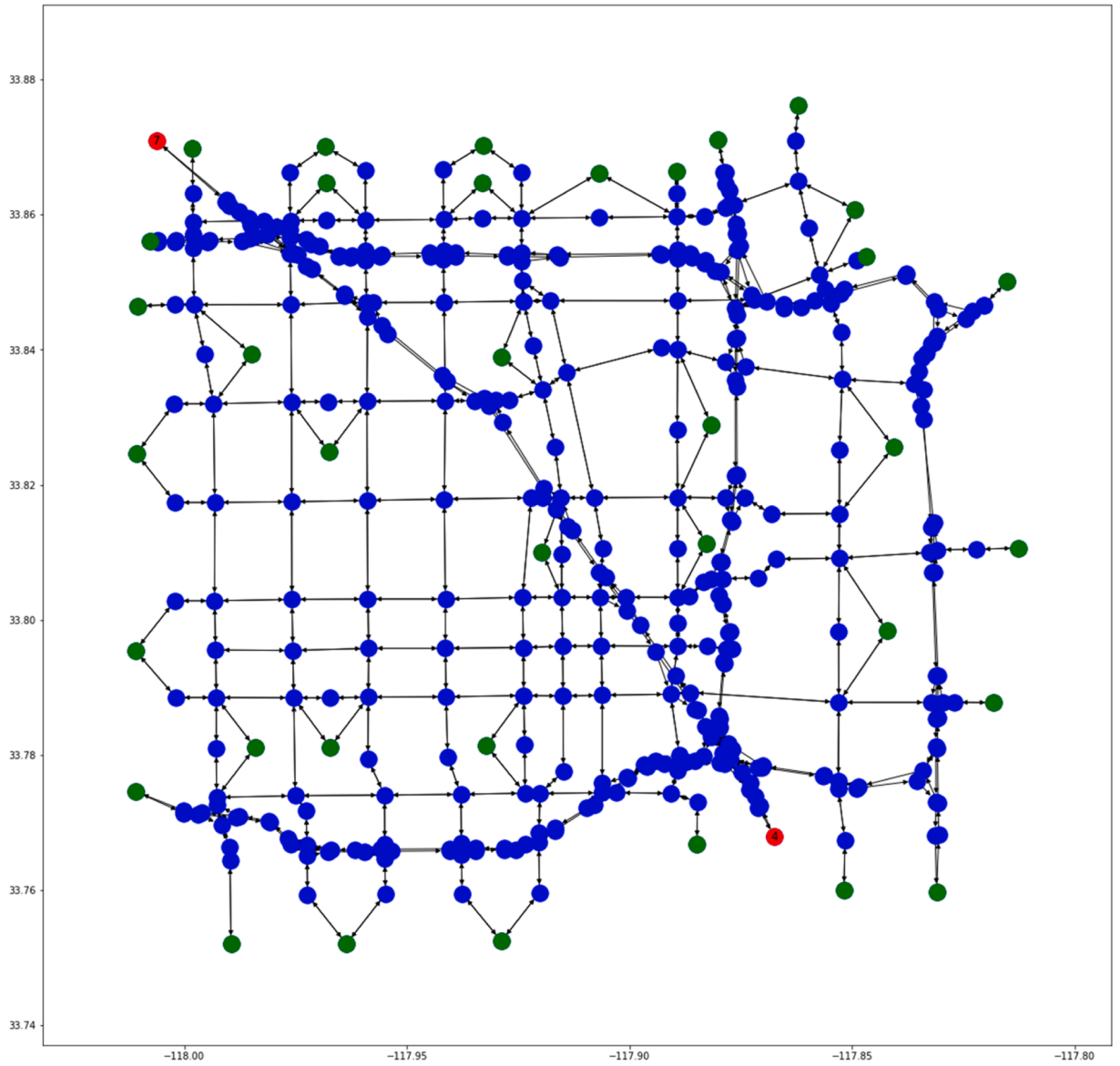

Fig. 13. Visual representation of the Anaheim network. Blue nodes constitute network nodes, green nodes constitute origin/destination nodes and red nodes are the origin/destination of the OD-relation we focus on for demonstration.

Proof. In general, if $W_1(\boldsymbol{t})$ and $W_2(\boldsymbol{t})$ are continuous functions in $\boldsymbol{t}$, then min $(W_1(\boldsymbol{t}),W_2(\boldsymbol{t}))$, max $(W_1(\boldsymbol{t}),W_2(\boldsymbol{t}))$, and $(W_1(\boldsymbol{t}))_+ =$ max $(W_1(\boldsymbol{t}),0)$ are all also continuous. It follows from this that $P_{mi}(\boldsymbol{t})$ in (17) is continuous in $\boldsymbol{t}$. It is clear that $H_{mi}(\boldsymbol{x})$ is continuous for all $\boldsymbol{x} \in G$ if $P_{mi}(\boldsymbol{t}(\boldsymbol{\Delta x}))$ as defined in (17) is a continuous function for all $\boldsymbol{x} \in G$. Thus, since $\boldsymbol{t}(\boldsymbol{\Delta x})$ is a continuous function for all $\boldsymbol{x} \in G$, and $P_{mi}(\boldsymbol{t}(\boldsymbol{\Delta x}))$ in (17) is continuous in $\boldsymbol{t}$, then $H_{mi}(\boldsymbol{x})$ is continuous for all $\boldsymbol{x} \in G$. ■

Given $\boldsymbol{H}(\boldsymbol{x})$ and Lemma 1, we can now prove that BCM-LDT SUE solutions are guaranteed to exist.

Proposition 1. If the link cost function $\boldsymbol{t}(\boldsymbol{\Delta x})$ is a continuous function for all $\boldsymbol{x} \in G$, then at least one BCM-LDT SUE fixed-point route flow solution $\boldsymbol{x}^* \in G$ is guaranteed to exist.

Proof. It is clear that a route flow vector $\boldsymbol{x}^*$ is a BCM-LDT-SUE solution iff $H_{mi}(\boldsymbol{x}^*) = x^*_{mi}, \forall i \in R_m$, $m = 1, \ldots, M$. From the assumption that $\boldsymbol{t}(\boldsymbol{\Delta x})$ is a continuous function for all $\boldsymbol{x} \in G$, and thus from Lemma 1 $\boldsymbol{H}(\boldsymbol{x})$ is also a continuous function for all $\boldsymbol{x} \in G$, then since G is a nonempty, convex, and compact set, and $\boldsymbol{H}$ maps G into itself, then by Brouwer's Fixed-Point Theorem at least one solution $\boldsymbol{x}^*$ exists such that $\boldsymbol{H}(\boldsymbol{x}^*) = \boldsymbol{x}^*$, and hence BCM-LDT SUE solutions are guaranteed to exist. ■

Note that standard proofs for proving uniqueness of fixed-point solutions do not apply to the BCM-LDT SUE model. That is not to say, however, that solutions are not unique, merely a suitable proof has not yet been identified. Indeed, after investigating in a series of

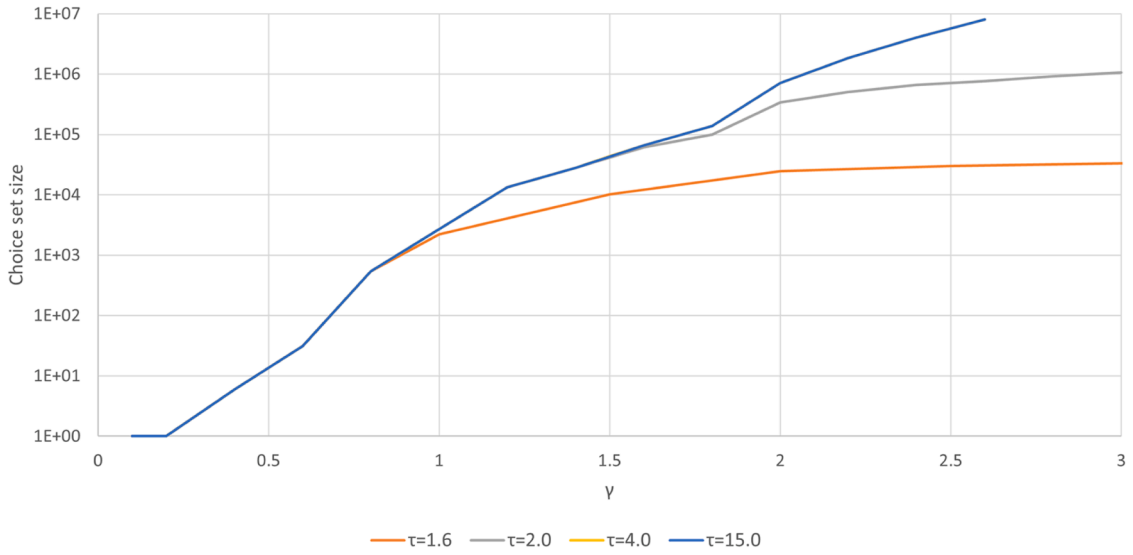

Fig. 14. Anaheim network: Choice set size as function of γ for various values of τ. Note the log-scale on the vertical axis, and also that curves for $\boldsymbol{\tau} = \{4.0, \quad 15.0\}$ are on top of each other in this range. Origin node: 4, Destination node: 7.

experiments, no cases of multiple solutions have been found (under the usual assumptions of monotonically increasing and separable travel time functions).

5.2. Solution algorithm

A novel solution algorithm is proposed that exploits the special structure of the problem, namely that all and only routes below the cost bound and local detour threshold are assigned non-zero flows at equilibrium. A particularly important part of the method is the use of a branch-and-bound algorithm to efficiently generate all routes satisfying the local detour threshold and global cost bound. Essentially, there are four elements of the algorithm which are iteratively performed:

- *Column generation* (branch-and-bound): Identify all routes with a local detouredness measure less than γ and a relative surplus total route cost less than τ.
- *Flow allocation*: Use choice probabilities to infer auxiliary route flows, and use flow averaging to combine with those determined in the previous iteration.
- *Removal of bound/threshold violations:* For any routes violating the local detour threshold or global cost bound, redistribute their flow to routes under the threshold/bound.
- *Network loading:* Calculate revised link costs based on the current flow allocation.

The algorithm, summarised as pseudo-code in Algorithm 1, was implemented in Java (no license is required). We have made this code available on GitHub https://github.com/tkra-dtudk/BCMLDT. Here we provide some more details of the steps involved.

In the Column Generation (Steps 0 and 4), the branch-and-bound algorithm is implemented as a modified Depth-First Search Algorithm, in which the list of visited nodes are stored in order to generate the resulting routes (Cormen et al., 2009, Chapter 22). The algorithm is applied for each Origin-Destination movement. It creates branches (i.e. sequence of nodes) from the origin, which branch off at nodes to eventually form routes when the destination is reached. The branches are bounded along the way, however, to ensure that the routes formed are those that satisfy the local detour threshold and global cost bound criteria. The bounding consists of performing the following checks when considering the extension of a branch to a currently unvisited node:

i) Is the current distance (in cost) along the branch to the unvisited node plus the shortest distance (in cost) from the unvisited node to the destination above the cost bound? If so, stop searching along this branch, and continue to next unvisited branch.
ii) Is the local detouredness between the unvisited node and any previous node in the branch above the local detour threshold? If so, stop searching along this branch, and continue to next unvisited branch.

If both the cost bound and local detour threshold are not violated during these checks, the node is added to the branch. The final result is that upon pruning the violating branches, and thus the possible routes stemming from those branches, the branch-and-bound algorithm generates all the routes that do not violate either the global cost bound or local detour threshold. Moreover, the local detouredness measure of each generated route is calculated along the way. It is determined as the maximum of the largest local detouredness calculated in ii) and the local detouredness measure determined for the previous node in the branch. When the

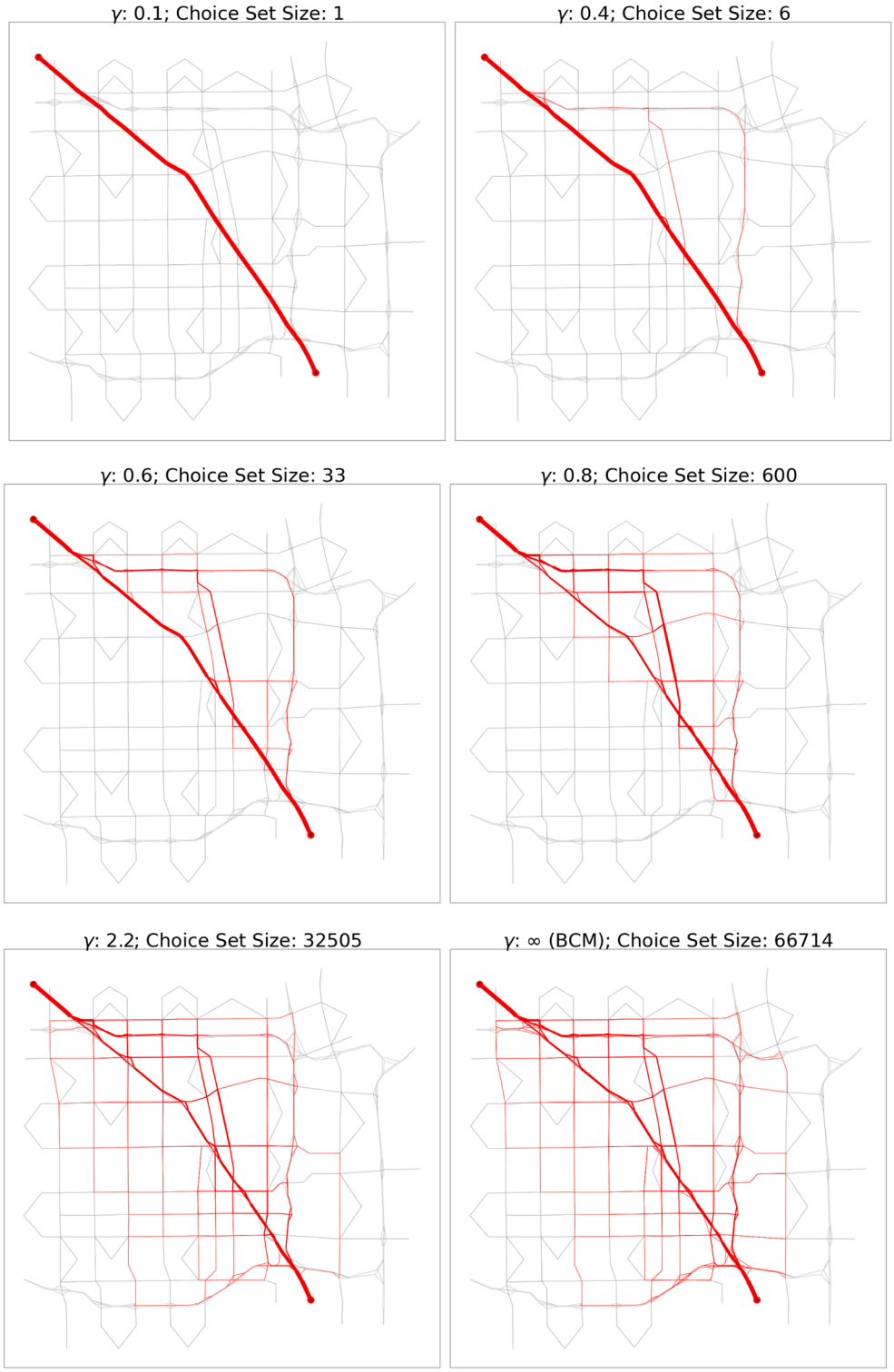

Fig. 15. Anaheim network: BCM-LDT link probabilities for different values of γ (including infinite γ, collapsing the BCM-LDT to the cost-BCM), assuming $\tau = 1.6$. The width of a link indicates its link probability. Origin node: 4, Destination node: 7.

destination is reached, this determines the local detouredness measure of the route.

Note that both i) and ii) use shortest path distances (costs) between nodes, namely between origin and destination and between unvisited node and destination for i), and between unvisited node and previously visited nodes in the branch for ii). Rather than

Algorithm 1
Pseudo-code, solving BCM-LDT SUE.

Step 0	*Initialisation:* For all OD movements $m = 1, \ldots, M$, enumerate initial choice sets using branch-and-bound approach based on free-flow link travel costs, and given the global bound and local detour threshold parameters τ and γ. Calculate initial route flows $\mathbf{x}^{(0)}$ using free flow travel costs, i.e. $x_{mi}^{(0)} = d_m P_{mi}(\mathbf{t}(\Delta 0))$, $\forall i \in R_m$, $m = 1, \ldots, M$. Perform network loading to compute the link travel costs $t_a^{(0)}\left(\mathbf{\Delta x}^{(0)}\right)$ on all network links $a = 1,2, \ldots,$A. Set $n = 1$.
Step 1	*Flow allocation:* Compute the auxiliary route flow $\bar{x}_{mi}^{(n)} = d_m P_{mi}\left(\mathbf{t}^{(n-1)}\right)$ and perform flow averaging $x_{mi}^{(n)} = (1 - \lambda_n) \cdot x_{mi}^{(n-1)} + \lambda_n \cdot \bar{x}_{mi}^{(n)}$ for all routes $i \in R_m$ for all *OD-pairs M*.
Step 2	*Bound or Threshold violation:* For each OD movement $m = 1, \ldots, M$, check for all routes $i \in R_m$, if $\bar{x}_{mi}^{(n)} = 0$ and $x_{mi}^{(n)} > 0$ (i.e. whether any used route is assigned zero auxiliary flow, implying violation of cost bound and/or local detour threshold). Redistribute the sum of all violating route flows $x_{mi}^{(n)}$ for OD movement m among the non-violating route flows, according to BCM-LDT choice probabilities $\boldsymbol{P}_m(\mathbf{t}^{(n-1)})$: $x_{mj}^{(n)} = x_{mj}^{(n)} + P_{mj}\left(\mathbf{t}^{(n-1)}\right) \cdot \sum_{i \in R_m:\ \bar{x}_{mi}^{(n)} = 0} x_{mi}^{(n)}, \forall j \in R_m :\ \bar{x}_{mj}^{(n)} > 0.$
Step 3	*Network Loading:* Perform network loading to obtain $\mathbf{x}^{(n)}$. Compute link travel costs $\mathbf{t}^{(n)}(\mathbf{\Delta x}^{(n)})$.
Step 4	*Column generation phase:* For all OD movements $m = 1, \ldots, M$, perform a branch-and-bound search based on the current link costs and bound parameters to generate all the routes satisfying the current local detouredness threshold and global cost bound (see description above). Compare to existing enumerated choice sets, if new unique routes are generated, add them to the corresponding choice sets with flow $x_{mi}^{(n)} = 0$.
Step 5	*Convergence:* Compute $RMSE^{(n)}$. If $RMSE^{(n)} < 10^{-\zeta}$ and no additional routes were added in *Step 4* stop. Else set n=n+1 and return to *Step 1*.

performing these shortest path searches along the way, we instead, to be more efficient, initialise the branch-and-bound algorithm by first identifying shortest cost distances between all node-pairs, so that these are at hand (i.e. memoisation). Also note that ii) does not necessarily involve checking the local detour between the node under investigation and *all* previous nodes visited in the branch, since the checks can stop when a violation of the detour threshold is found.

Turning to the other steps of the algorithm, the flow averaging in Step 1 adopted the Method of Successive Weighted Averages (MSWA) proposed by Liu et al. (2009), with the step-size λ_n at iteration n given by:

$$\lambda_n = \frac{n^z}{\sum_{k=1}^{n} k^z},$$

where $z \geq 0$ is the MSWA parameter. Increasing the value of z moves more flow towards the auxiliary solution, and the MSWA collapses to the well-known Method of Successive Averages (MSA) when $z = 0$. In Liu et al. (2009) it is shown that the MSWA guarantees the convergence of the SUE problem regardless of z (as long as it is greater than or equal to zero and not necessarily an integer).

In Step 2, the flows on routes violating the local detour threshold / global cost bound are redistributed among routes not violating the threshold/bound. There are multiple ways in which this could be done, e.g. redistribute flow from only one route (e.g. the most violating route) at each iteration, or to redistribute the sum of flows on all violating routes to the non-violating ones. We adopted the latter approach, redistributing to non-violating routes according to their current auxiliary probabilities. This way, non-violating routes with costs / detour measures close to the bound/threshold should receive only small shares of the redistributed flow. This reduces the likelihood of them consequently violating the new bound/threshold, if the costs / detour measures were recomputed and the routes were re-checked. It is important to note, however, that it is not necessary to re-check for new violating routes and to redistribute again in the current iteration until all routes satisfy the bound/threshold criteria, as the new violating routes will be addressed in the following iteration, and the problem will be resolved at convergence. Thus, either all or the Z most violating routes could be redistributed at each iteration, and in the end the costs and detour measures from the flows will satisfy the bound/threshold criteria. In our experiments, we did not find any issues related to this, as we found no violating routes used at convergence.

In Step 3, the network link costs are then updated; Step 4 has been discussed above. In Step 5, if no additional routes are generated in Step 4 and the Route Mean Squared Error (RMSE) between the final route flow vector and auxiliary route flow vector at iteration n is below a certain value, the algorithm is considered to have converged to a BCM-LDT SUE solution. The RMSE is computed as:

$$RMSE^{(n)} = \sqrt{\frac{1}{N} \sum_{m=1}^{M} \sum_{i \in R_m} \left(x_{mi}^{(n)} - \bar{x}_{mi}^{(n)}\right)^2},$$

where $x_{mi}^{(n)}$ and $\bar{x}_{mi}^{(n)}$ are the final route flow and auxiliary route flow for route $i \in R_m$ at iteration n. The route flows are thus said to have converged sufficiently to a route flow vector solution $\boldsymbol{x}^* = \boldsymbol{x}^{(n)}$ if $RMSE^{(n)} < 10^{-\zeta}$, where ζ is a predetermined flow convergence parameter.

In the BCM-LDT SUE solution algorithm in Algorithm 1, it is stipulated, for generality, that a column generation phase is adopted at every iteration. However, it is not necessary to do this at every iteration, and, dependent on the case, it may be beneficial computationally to do this e.g. at every k iterations. Moreover, it may also be beneficial to generate larger choice sets initially in Step 0, for example by adding a value of ς to the local detour threshold γ and global cost bound τ. This is in order to begin with a larger working route set that will likely cover all the main routes required; it is a recognition of the inaccuracy of the initial travel costs, which are set to free-flow values. Our numerical experience was that initiating with larger choice sets indeed expedited the overall convergence of the method.

5.3. Numerical experiments

In this section we demonstrate the properties of the BCM-LDT in an equilibrium setting.

5.3.1. 3-route simple network

We now demonstrate the BCM-LDT in an equilibrium setting on a simple three route network. We will compare BCM-LDT SUE with two alternative ways one might have approached the consideration of thresholds on local detours. This will highlight the importance of the need to consider congestion effects when deciding the composition of the choice set, as well as the importance of incorporating the local detour threshold as part of the choice probability expression rather than a hard constraint. We will compare the following three approaches: (i) an initial removal of local detour routes strictly based on free-flow costs, and then an application of the standard cost-BCM SUE (Watling et al., 2018) on the resulting choice set (Model 1), (ii) applying the standard cost-BCM SUE, but with an additional hard constraint requiring used routes to not violate a detouredness threshold (Model 2), (iii) the formulated BCM-LDT SUE conjunctive choice model (Model 3).

Assume the same 3 route network structure as used for the illustrative example in Section 4.4, i.e. as in Fig. 16 below. Define Route 1 as consisting of links 1 and 3, Route 2 as consisting of links 1 and 2, and Route 3 as consisting of link 4.

Now, assume the link costs are now flow-dependent, i.e.

$$t_a = t_{0a} + \left(\frac{f_a}{C_a}\right)^2$$

With free-flow travel times $\boldsymbol{t}_0 = (50, \quad 10, \quad 5, \quad 50)$, capacities $\boldsymbol{C} = (1000, \quad 1000, \quad 100, \quad 1000)$, and a total demand of d=5000 units travelling through the network. In the analysis we assume a travel cost scaling parameter $\theta_1 = 0.01$ and $\tau = 1.3$ for the cost-BCM in Models 1&2 and the cost-BCM part of the BCM-LDT in Model 3. For the BCM-LDT, we assume $\theta_2 = 1.0$ and $\gamma = 0.5$, and in Models 1&2 we assume a local detour route cut-off of 0.5.

Table 2 displays results from applying each of Models 1-3 to the small-scale network.

Model 1 corresponds to the situation where travellers exclude alternatives with long local detours based on fixed free-flow costs. In free-flow conditions, the detouredness of Routes 1, 2, and 3 are 0.1, 1.0, and 0.0, respectively. As such, Model 1 will not utilise Route 2, and identifies a cost-BCM solution in which Routes 1 and 3 are used. Thereby we get existence of solutions, since all we are doing is refining the initial – fixed – permitted choice set and then applying the cost-BCM SUE. However, looking at the results in Table 2, it can be seen that at equilibrium, the initially rejected route is less costly than the cheapest used route and has the lowest local detour measure among all routes. A solution without this used route is arguably behaviourally unrealistic.

Model 2 may result in non-existence of solutions, as demonstrated by the results shown in Table 2. As can be seen, Route 1 violates the local detour cut-off. Furthermore, although another flow distribution (among the three routes or a subset of routes) may fulfil the local detour cut-off, it would not be a cost-BCM SUE solution since this is unique. Thus, no solutions exist. Note that while no solutions exist for Model 2 in the case above, this is not the case in general. For example, if the local detour route cut-off had been set at 0.7, then a solution would exist (the one presented in the table). Model 2 thus alludes to the need for considering the local detour cut-off as part of the (continuous) choice probability model.

Model 3 provides guaranteed solution existence (as proven in Section 5.1). In this example, flow is distributed between all three routes at equilibrium, without the local detour threshold nor global cost bound being violated. For reference, the MNL SUE is also shown in the table. This distributes flow to all three routes, as expected, but with a relatively large share of flow to Route 2 that, given the current parameter settings, has a very large local as well as global detour.

5.3.2. Anaheim network

In the following we apply Algorithm 1 to solve BCM-LDT SUE on the Anaheim network. The initial SUE conditions are set as the BCM-LDT route flows using free flow travel costs, i.e. $x_{mi}^{(0)} = d_m P_{mi}(\mathbf{t}(\boldsymbol{\Delta}0)), \forall i \in R_m, m = 1, \ldots, M$, and the RMSE route flow convergence parameter is set as $\zeta = 5$. After some preliminary experiments, we chose to set the MSWA parameter as $z = 2$ as this seemed to provide suitably fast convergence rates. Unless stated otherwise, the BCM-LDT parameters are set as $\theta_1 = \theta_2 = 0.2$, $\tau = 1.6$, and $\gamma = 0.8$. As per the discussion at the end of Section 5.2, in Step 0 of Algorithm 1 we added $\varsigma = 0.4$ to the local detour threshold and global cost bound parameters. This was sufficiently large to ensure that it was – for the current case study – not necessary to perform additional branch-and-bound searches in *Step 4* of the solution algorithm with iterating towards convergence (corresponds to setting k infinitely large). Upon termination, it was checked whether any additional relevant routes had not been initially generated.

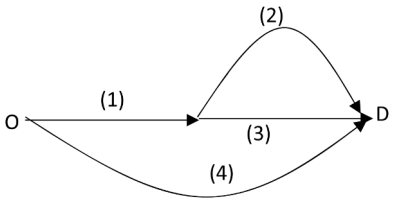

Fig. 16. Small-scale network. 4 link network with 3 routes from origin O to destination D. Numbers () identify link number.

Table 2
Small-scale network: Converged flow solution for various different models and allowed choice sets. Cost bound: $\tau = 1.3$, detour threshold/cut-off: $\gamma = 0.5$.

Model	Allowed	x_i			c_i			Global detour			Detouredness ϕ_i		
		R1	R2	R3	R1	R2	R3	R1	R2	R3	R1	R2	R3
1	[1,0,1]	568.1	-	4431.9	87.6	60.3	69.6	1.45	1	1.15	2.73	0.0	0.15
2	[1,1,1]	388.7	1620.4	2990.9	74.1	66.7	58.9	1.26	1.13	1.0	0.59	0.13	0.0
3	[1,1,1]	340.2	1528.7	3131.1	70.1	65.8	59.8	1.17	1.1	1.0	0.34	0.1	0.0
MNL	[1,1,1]	904.2	1880.5	2215.3	144.5	71.3	54.9	2.63	1.3	1.0	5.41	0.3	0.0

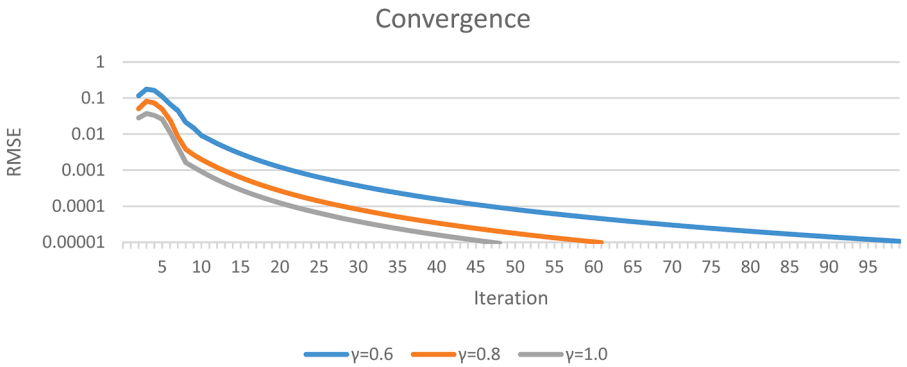

Fig. 17. Anaheim network: Convergence pattern of BCM-LDT SUE for various values of γ, assuming $\boldsymbol{\theta}_1 = \boldsymbol{\theta}_2 = 0.2$, $\boldsymbol{\tau} = 1.6$.

5.3.2.1. Convergence. Fig. 17 illustrates the convergence pattern (RMSE) as a function of iteration number for three different settings of the local detour threshold parameter γ. Notice the log-scale on the vertical axis. As can be seen, the algorithm converges smoothly to a highly converged BCM-LDT SUE solution. The number of iterations needed increases with decreasing γ. This is because the threshold is tighter, causing smaller choice sets and thereby larger fluctuations in flow and thus travel time between iterations. The computation time is highly dependent on γ, with each iteration of the algorithm taking on average 1.5, 8, and 180 minutes when γ is 0.6, 0.8, and 1.0, respectively in the current implementation. This is caused by the non-linear increase in the choice set size with γ, as shall be explored in the section below.

5.3.2.2. Choice set analysis. Fig. 18 illustrates the cumulative distribution of the size of the equilibrated choice sets of used routes for various values of γ, while Fig. 19 illustrates the average choice set size for various values of γ.

As can be seen from Fig. 18, the choice set sizes of used routes are highly dependent on γ. While the median choice set size is generally low across all tested γ (median = 3, 5, 29, 84, 185 for γ = 0.2, 0.3, 0.6, 0.8, 1.0 respectively), there can be a large variation across the different OD-relations. For large γ for some OD-pairs the choice sets become very large, containing more than 50,000 alternatives (though still much smaller than the universal choice set of simple paths). With $\gamma = 0.2$ there are relatively few OD-pairs with more than 500 used routes (<1 % of OD-relations), whereas this share is much larger for γ =1.0 (40 % of OD-relations). The skewed distribution of the number of routes across the OD-relations naturally implies that the mean choice set size is larger than the median, especially so for high values of γ. From Fig. 19 it can be seen that the number of used routes decreases rapidly with decreasing γ, and so

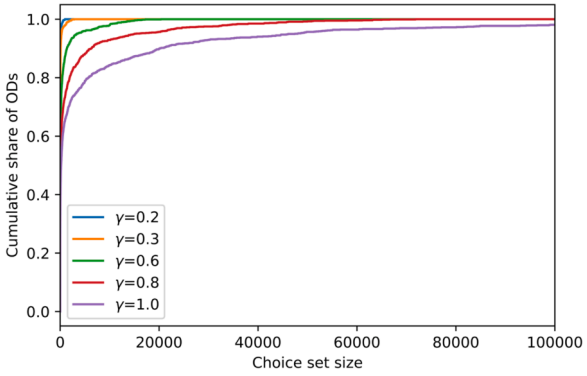

Fig. 18. Anaheim network: Distribution of choice set size at various values of γ. Left: x-range to 100,000; Right: x-range to 20,000. Assuming $\boldsymbol{\theta}_1 = \boldsymbol{\theta}_2 = 0.2$, $\boldsymbol{\tau} = 1.6$.

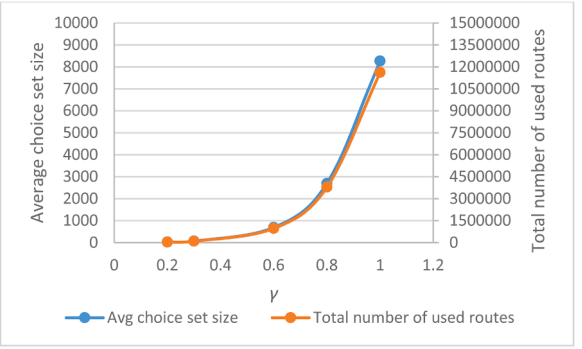

Fig. 19. Anaheim network: Average choice set size and total number of used routes at various values of γ. Assuming $\theta_1 = \theta_2 = 0.2$, $\tau = 1.6$.

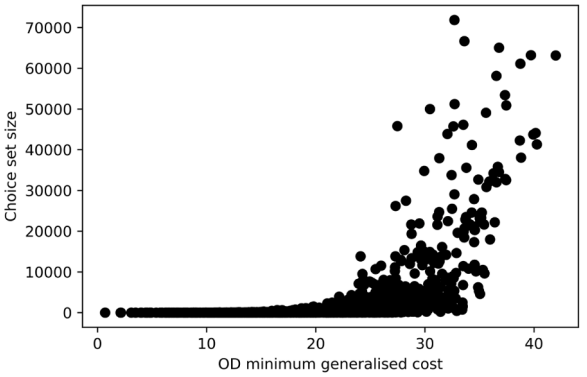

Fig. 20. Anaheim network: BCM-LDT SUE equilibrated choice set sizes as function of OD minimum generalised cost, assuming $\theta_1 = \theta_2 = 0.2$, $\tau = 1.6$, $\gamma = 0.8$.

from a computational point of view it is attractive to have a low γ. However, γ needs to be calibrated from real data, and we have shown that (at least for the network considered) the approach is computationally tractable even for large values of γ.

The remainder of the analysis will focus on γ=0.8. As illustrated in Fig. 20, the choice set size is greatly dependent on trip cost, where more costly trips can have significantly larger choice sets. Looking again at the OD-movement from Origin 4 to Destination 7, there are 351 unique alternatives active (used) in the equilibrated solution. Fig. 23A illustrates the resulting choice probabilities on the routes, as a function of their local detouredness measure and relative global detour. As can be seen, no active routes violate the threshold on local detour as well as the cost bound, and choice probability is, as expected, reduced for increasing local detour as well as cost. The route with highest probability is the main motorway alternative with zero detouredness and a relative cost of 1.0. Note that, the impact of the cost-BCM (Q^1_{mi}) contribution to overall BCM-LDT probability can be seen as the change in probability when the relative global detour changes but the local detouredness is kept constant (corresponds to moving horizontally in the Fig.). This is also the case for the detour-BCM (Q^2_{mi}) contribution, vertically.

5.3.2.3. Flow distribution. Fig. 21 illustrates the equilibrated flow on the network links across all OD-relations. Overall, the flow distribution seems plausible with most flows on the highest-class main motorway I-5, less flow on State Routes such as SR-22, and least flow on minor roads.

Fig. 22 illustrates the link flow difference between the DUE solution (obtained by solving BCM-LDT SUE with $\gamma \cong 0$ and $\tau \cong 1$) and the BCM-LDT SUE solution with $\gamma = 0.2$ and $\gamma = 0.8$. As expected, the flows are allocated to more routes under BCM-LDT SUE than DUE – only the minimum costing routes are used in DUE, while all routes within the cost bound and local detour threshold are used in BCM-LDT SUE. Consequently, the less costly motorways receive greater flows under DUE (as shown by the blue lines), and the more costly more minor roads receive greater flows under BCM-LDT SUE (as shown by the red lines). Small γ approximates DUE, where only the optimal routes are used, and greater values of the threshold γ increases the spread of the flows, assigning more routes with more flow.

As the local detour threshold – and cost bound – increase towards infinity, the BCM-LDT SUE solution approaches an MNL SUE solution where all available routes are used, and thus where the flows will be even more spread among motorways and minor roads. Since solving MNL SUE would require enumerating the universal choice set, which would not be computationally feasible on this network, we cannot provide a similar comparison to Fig. 22 between MNL SUE and BCM-LDT SUE. One could provide a comparison with MNL SUE with pre- or column-generated approximated universal choice sets, but we have already established the inconsistencies of that approach (see Section 1 of the present paper and Watling et al. (2018)).

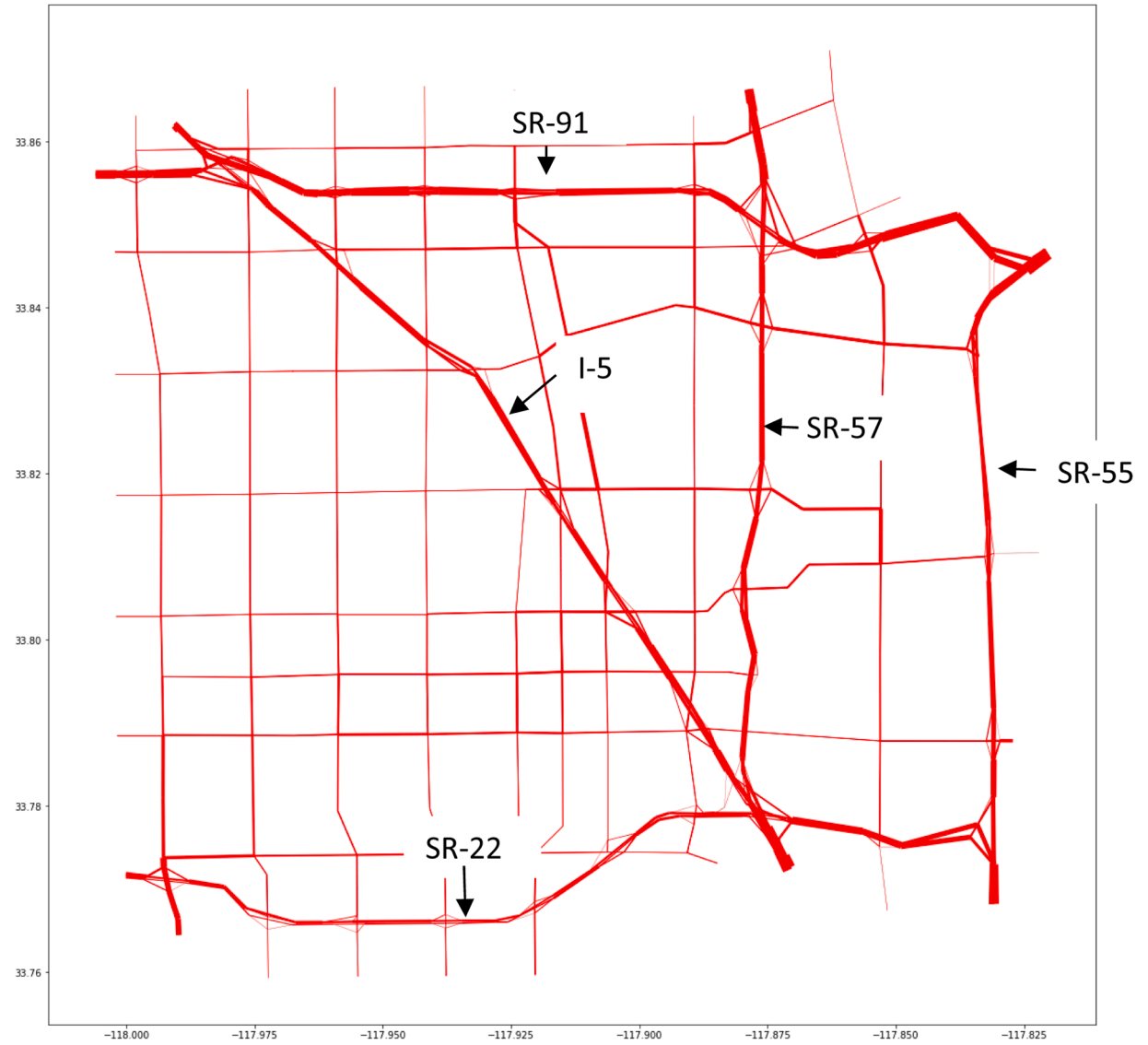

Fig. 21. Anaheim network: BCM-LDT equilibrated flow solution with line width indicating flow share, assuming $\boldsymbol{\theta}_1 = \boldsymbol{\theta}_2 = 0.2$, τ=1.6, γ=0.8. Connectors have been removed from the illustration.

Note that it is also not computationally attractive to solve the standard cost-BCM SUE on this network, as the route choice sets for even moderate sizes of the global bound are very large, see for example Fig. 15 with local detour threshold $\gamma = \infty$, where 66,714 routes are generated for that one OD with global bound $\tau = 1.6$. This weakness of the standard cost-BCM SUE was a key computational motivation for incorporating local detours into the choice model, aside from the behavioural reasons. Therefore, it is a key attractive feature of BCM-LDT SUE that it resolves this weakness, by being computationally feasible to solve with reasonable choice set sizes (that are consistent with the probability model).

5.3.2.4. Impact of the scaling parameters. As can be seen from (17), the θ_1 parameter scales sensitivity to travel cost relative to the global bound, i.e. θ_1 scales $c_{mi}(\boldsymbol{t}) - \tau \cdot \min \quad (c_{ml}(\boldsymbol{t}): l \in R_m)$. On the other hand, θ_2 scales sensitivity to local detouredness relative to the local bound, i.e. θ_2 scales $\phi_{mi}(\boldsymbol{t}) - \gamma$. Therefore θ_1 could be scaling any range of values, dependent on the magnitude of generalised costs in consideration (e.g. generalised minutes or hours), while θ_2 scales values between 0 and γ (typically around 0-3).

In this case study of Anaheim, θ_1 scales values between 0-35, and therefore θ_1 is scaling an overall greater magnitude of values. This suggests that in this case θ_1 should perhaps be smaller than θ_2, though this depends of course on the calibration to observed behaviour. In the prior numerical experiments, θ_1 was set to equal θ_2. We shall explore here the impact of decreasing θ_1 and keeping θ_2 the same, i.e. when setting $\theta_1 = 0.01$ and $\theta_2 = 0.2$ compared to $\theta_1 = \theta_2 = 0.2$.

Fig. 23B displays the corresponding Fig. to Fig. 23A, with $\theta_1 = 0.01$. As shown, although the values of relative global detour and

Fig. 22. Anaheim network. Left: Link flow difference between BCM-LDT SUE and DUE. Left: BCM-LDT SUE with γ=0.2. Right: BCM-LDT SUE with γ=0.8. Width indicates size of flow difference, with red/blue colour indicating more/less flow for BCM-LDT SUE than DUE. $\boldsymbol{\theta}_1 = \boldsymbol{\theta}_2 = 0.2$, $\boldsymbol{\tau} = 1$.

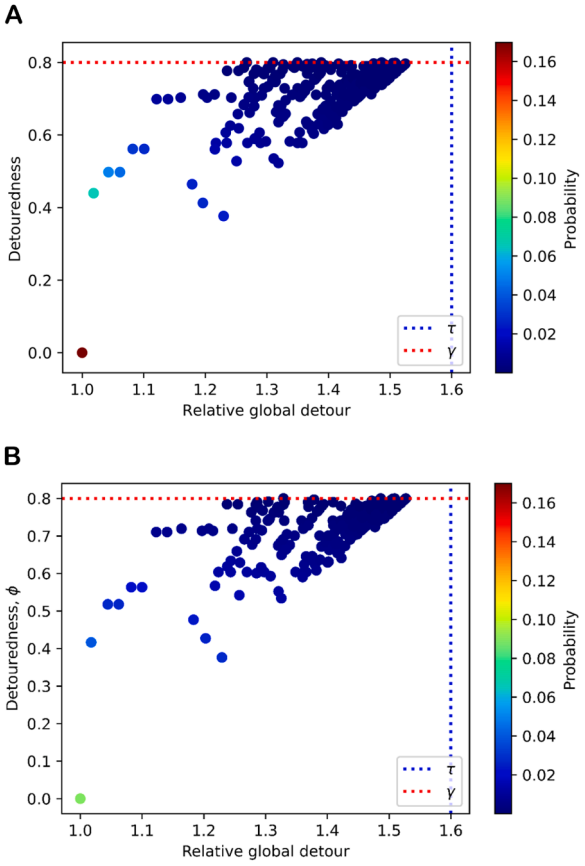

Fig. 23. Anaheim network: Route choice probability as function of global detour and local detouredness, at BCM-LDT SUE. Origin node: 4, Destination node: 7, assuming $\boldsymbol{\theta}_2 = 0.2$, $\boldsymbol{\tau} = 1.6$, $\boldsymbol{\gamma} = 0.8$. A: $\boldsymbol{\theta}_1 = 0.2$. B: $\boldsymbol{\theta}_1 = 0.01$.

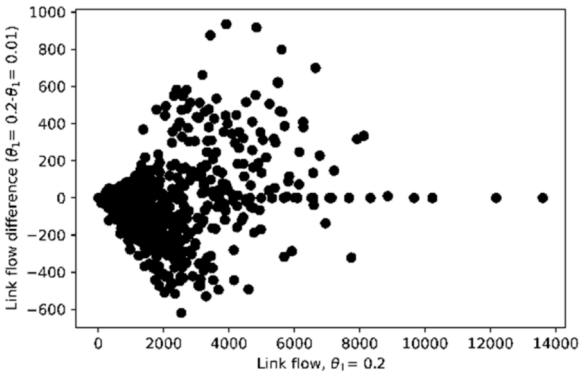

Fig. 24. Anaheim network: Differences in link flows between BCM-LDT SUE solution with $\boldsymbol{\theta}_1 = 0.2$ and $\boldsymbol{\theta}_1 = 0.01$.

local detouredness do not vary significantly, the choice probabilities of the routes do vary, as evident from the differing colours of the dots. Most notably, the shortest route with relative global detour of 1 and local detouredness of 0, changes from a dark red probability of 0.17 to a light green probability of 0.09. This is expected as the decrease in θ_1 implies lower sensitivity to differences in global travel cost, and the BCM-LDT choice probabilities consequently being more similar among used routes.

With this shift in route choice probabilities, we also expect the link flows to be different. Fig. 24 displays the differences in link flow between the BCM-LDT SUE solution with $\theta_1 = 0.2$ and $\theta_1 = 0.01$. As can be seen, the shift in route choice probabilities does indeed

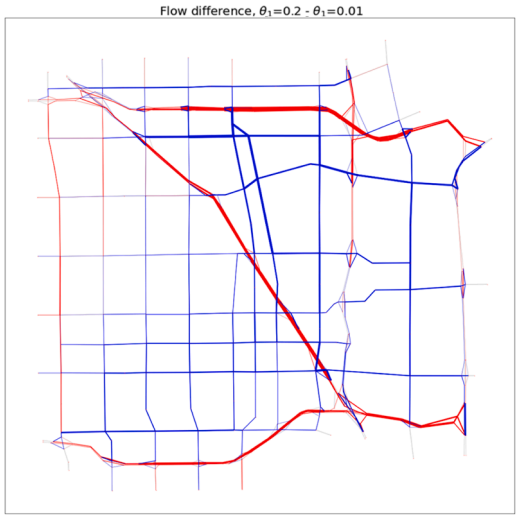

Fig. 25. Anaheim network: Difference in link flows between BCM-LDT SUE solution with $\boldsymbol{\theta}_1 = 0.2$ and $\boldsymbol{\theta}_1 = 0.01$, represented spatially, with red/blue indicating more/less flow for the $\boldsymbol{\theta}_1 = 0.2$ solution than the $\boldsymbol{\theta}_1 = 0.01$ solution. Link width indicates the size of the flow difference.

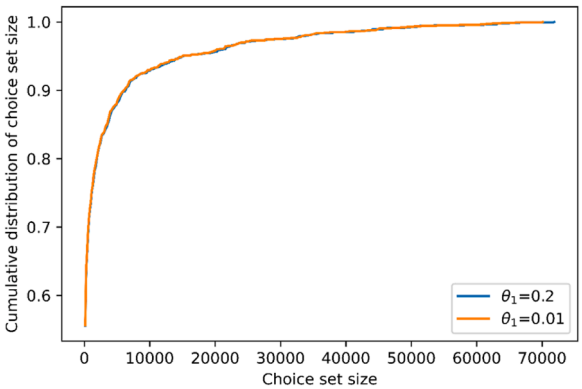

Fig. 26. Anaheim network: Cumulative distribution of choice set size upon equilibration of BCM-LDT SUE with $\boldsymbol{\theta}_1 = 0.2$ and $\boldsymbol{\theta}_1 = 0.01$.

impact the link flows, with more flow going to links with low flow levels ($x_a < 2500$) under $\theta_1 = 0.01$, and less flow going to links with medium flow levels ($2500 \leq x_a \leq 7000$) under $\theta_1 = 0.01$. Fig. 25 displays the differences in link flow spatially on the Anaheim network, where red/blue link colour indicates higher/lower link flow under BCM-LDT SUE with $\theta_1 = 0.2$ than with $\theta_1 = 0.01$, and the thickness represents the size of the difference. As shown, with $\theta_1 = 0.01$, there is greater flow on the minor roads. This is because these roads are often used by routes with higher costs, and $\theta_1 = 0.01$ assigns more probability and thereby more flow to these routes.

Lastly, to explore the impact on choice set composition, Fig. 26 displays the cumulative distribution of choice set size for $\theta_1 = 0.01$ and $\theta_1 = 0.2$. It can be seen that in spite of the earlier evidence of the impact of θ_1 on choice probabilities and link flow solutions, the differences in the composition of the choice sets are marginal between the two cases tested.

6. Conclusions

6.1. Discussion

In the introduction and motivation section of this paper, it has been illustrated theoretically and empirically that there is a need to consider the impact of local detours (i.e. detours on segments of a route), both when generating realistic and tractable route choice sets, as well as when determining route choice probabilities. However, prior to this study, no existing modelling approaches have accounted for local detours either in route generation methods or in the route choice model.

The current paper has addressed this by developing a new route choice model: the Bounded Choice Model with Local Detour Threshold (BCM-LDT) model, which has been carefully designed in order to achieve some desirable features:

- Local detouredness is an influencing factor upon route choice probability, where the route choice model considers local detouredness alongside total route travel cost.
- Local detouredness considers the extent to which travellers detour in terms of generalised travel cost, and thus local detouredness varies with travel cost parameters, link flows (in the case of congested flow-dependent link travel times), and policy attributes (e.g. toll price).
- The route choice model implicitly defines which routes are used and unused. Thus, upon solution of the model, the used route choice sets will be generated, and be consistent with the route choice probability criteria.
- The used route choice sets are determined by considering bounds travellers have both on total surplus route travel cost and local detouredness, so a route must satisfy both bounds to receive non-zero probability.
- The route choice probability function is closed-form and continuous, which also includes as routes go from used to unused, and vice versa, as e.g. flow/parameters are varied. Achieving this is not trivial, and makes the approach robust and well-behaved.

The paper then established Stochastic User Equilibrium conditions for the BCM-LDT, where equilibrium solutions were proven to exist. A corresponding solution algorithm was then developed that equilibrates the choice set of used alternatives simultaneously (and consistently) with the flow equilibration. The algorithm utilises the built-in feature of the model for distinguishing between used/unused alternatives, to generate consistent choice sets without the need to enumerate the universal set. This provides a major advantage over other existing approaches which either require enumerating the universal set (not feasible), or operating with generated choice sets, which – among other drawbacks – results in inconsistencies.

A novel branch-and-bound-based algorithm was proposed for determining all routes below the current cost bound and local detour threshold. Using this algorithm, illustrative examples were conducted on a small three-route network and the Anaheim network. On the three-route network we illustrated the well-behaved properties of the BCM-LDT SUE model compared to possible alternative naïve approaches. On the Anaheim network the proposed solution algorithm was found to have well-behaved convergence properties. Furthermore, it was shown that the choice set sizes are greatly dependent on (i.e. increase exponentially with) the local detour threshold, so that a tight threshold can significantly decrease the number of used routes. This highlights one of the strengths of the model compared to a standard cost-BCM / non-bounded SUE models.

It should also be noted that the BCM-LDT SUE model has significant flexibility. For different configurations of the parameters, the model can approximate both Deterministic User Equilibrium and Multinomial Logit SUE (in terms of travel cost and/or detouredness), i.e. traffic equilibrium models at the two different ends of the choice set size scale (i.e. only minimum cost routes / all possible routes).

6.2. Future research

Future research could explore estimating the BCM-LDT model, both in simulation experiments to assess whether assumed true model parameters can be reproduced, and fitting the model to real-life tracked route observations. This will provide further empirical evidence to support the model, and calibrate the local detour threshold parameter according to observed behaviour. Moreover, it will validate that local detouredness is an influencing factor upon route choice probability. Future research could also explore whether the local detouredness measure or local detour threshold should be dependent on total trip length/cost, for example to assess whether travellers on a longer trip are more or less willing to take a longer (relative) detour.

In these calibration efforts, we believe that new data sources deserve special attention, especially those that provide real-life tracked route observations such as GPS data (e.g., Prato et al. 2014, 2018; Łukawska et al., 2023), mobile phone data (e.g., Huang et al., 2018; Calabrese et al., 2013), automatic number plate recognition data (e.g., Siripirote et al., 2014; Mirzahossein et al., 2021) and Bluetooth data (e.g., Crawford et al., 2018; Delafontaine et al., 2012). We believe these sources to be particularly relevant to our

proposed model as they provide a sufficient level of detail to uncover the bounds that travellers actually consider, which would be hard to reveal with traditional link-level data, e.g. from loop detectors. Such route-level data is thus more valuable, we believe, even in small volumes (e.g. from a sample of users who agree to use of such tracking data), rather than high volumes of low-level data such as that from link flows. Combined with these emerging data sources, we have the potential for using many different estimation methods, such as special-purpose maximum likelihood estimators (e.g., Duncan et al., 2022a; Mohammadpour & Frejinger, 2022), methods utilising machine learning approaches (e.g., Kim et al., 2022; Liu et al., 2023), or Bayesian estimation methods (e.g., Huang et al., 2023; Wei & Asakura, 2013). These latter citations use route-level information to reveal network mobility patterns/parameters, and so provide a promising starting point for the estimation of our proposed model.

There is also significant scope for developing other solution algorithms that can solve the BCM-LDT SUE model more efficiently, such as developing more efficient methods for enumerating all routes that satisfy the bound and threshold, as well as calculating the detour ratio of the generated routes. For example, detours on sub-routes could be used to identify violating segments and calculate detour measures across many routes sharing the same sub-routes.

As discussed in the paper, while the BCM-LDT does take into account the overlap between routes, it does it from a local detour perspective. As was shown, this is very different to considering the overlap between routes from a correlation perspective. Future research could therefore explore how to extend the BCM-LDT to also account for route correlation. For example, by taking inspiration from how Duncan et al. (2022a) extend the standard cost-BCM to capture used route correlation, developing the Bounded Path Size route choice model.

While the 'aspects' we consider within the CBCM in the present study are total route cost and local detouredness, a wide range of aspects could alternatively/also be considered. For example, for bicycle route choice, there may be a bound upon slope or energy expenditure a cyclist is willing to consider, or for public transport a bound upon number of transfers, waiting time, etc,. In a traffic equilibrium context, there is potential to apply the CBCM to route choice situations involving multiple aspects including travel time reliability, charging anxiety for electric vehicles, and road pricing.

A main motivation for developing traffic assignment models is to apply them for policy analysis. This is where the true benefits of the BCM-LDT become evident, where the route choice sets being able to change according to policy changes (e.g., tolling), in a consistent and well-behaved way, is highly attractive. This distinguishing feature sets it apart from other models, and the implication of this on the outcome of policy analysis would be interesting to study in future research.

CRediT authorship contribution statement

Thomas Kjær Rasmussen: Writing – review & editing, Writing – original draft, Visualization, Software, Methodology, Investigation, Funding acquisition, Formal analysis, Data curation, Conceptualization. **Lawrence Christopher Duncan:** Writing – review & editing, Writing – original draft, Methodology, Investigation, Funding acquisition, Formal analysis, Data curation, Conceptualization. **David Paul Watling:** Writing – review & editing, Methodology, Formal analysis, Conceptualization. **Otto Anker Nielsen:** Writing – review & editing, Methodology, Conceptualization.

Declaration of competing interest

None.

Data availability

Software code made available on GitHub, GPS trajectories cannot due to privacy.

Acknowledgement

We gratefully acknowledge the financial support of the Independent Research Fund Denmark to the projects "Next-generation route choice models for behavioural realism and large-scale applications" [Grant ID: 0136-00242B] and "Optimal tolls for reaching emissions goals: A novel behaviourally realistic and national-scale applicable road transport modelling system" [Grant ID: 0217-00173B].

References

Bar-Gera, H., 2010. Traffic assignment by paired alternative segments. Transport. Res. Part B Methodol. 44 (8-9), 1022–1046.
Bazaraa, M.S., Sherali, H.D., Shetty, C.M., 2013. Nonlinear programming: theory and algorithms. John Wiley & Sons.
Bekhor, S., Prashker, J., 1999. Formulations of extended logit stochastic user equilibrium assignments. In: Proceedings of the 14th International Symposium on Transportation and Traffic Theory. Jerusalem, Israel, pp. 351–372.
Bekhor, S., Ben-Akiva, M.E., Ramming, S., 2006. Evaluation of choice set generation algorithms for route choice models. Ann. Oper. Res. 144 (1), 235–247.
Bell, M.G., Shield, C.M., Busch, F., Kruse, G., 1997. A stochastic user equilibrium path flow estimator. Transport. Res. Part C Emerg. Technol. 5 (3-4), 197–210.
Ben-Akiva, M., Ramming, S., 1998. Lecture notes: discrete choice models of traveler behavior in networks. *Prepare.* Adv. Methods Plann. Manage. Transport. Netw. *Capri, Italy*.
Ben-Akiva, M., Bergman, M.J., Daly, A.J., Ramaswamy, R., 1984. Modelling inter urban route choice behaviour. In: Papers presented during the *Ninth International Symposium on Transportation and Traffic Theory held in Delft the Netherlands*, 11-13 July 1984.
Bierlaire, M., 1998. Discrete choice models. Oper. Res. Dec. Methodol. Traffic Transport. Manage. 203–227.

Calabrese, F., Diao, M., Di Lorenzo, G., Ferreira, J., Ratti, C., 2013. Understanding individual mobility patterns from urban sensing data: A mobile phone trace example. Transport. Res. Part C Emerg. Technol. 26, 301–313.
Cascetta, E., Nuzzolo, A., Russo, F., Vitetta, A., 1996. A modified logit route choice model overcoming path overlapping problems: specification and some calibration results for interurban networks. In: Proceedings of the 13th International Symposium on Transportation and Traffic Theory. Lyon, France, pp. 697–711.
Cazor, L., Watling, D.P., Duncan, L.C., Nielsen, O.A., Rasmussen, T.K., 2024. A novel choice model combining utility maximization and the disjunctive decision rule, application to two case studies. (Paper currently under review).
Cormen, T., Leiserson, C., Rivest, R., Stein, Stein, 2009. ntroduction to algorithms, third edition. I. The MIT Press, One Rogers Street, Cambridge. MA 02142-1209. 2009. ISBN: 9780262033848.
Crawford, F., Watling, D.P., Connors, R.D., 2018. Identifying road user classes based on repeated trip behaviour using Bluetooth data. Transport. Res. Part A Policy Pract. 113, 55–74, 2018.
Daganzo, C.F., Sheffi, Y., 1977. On stochastic models of traffic assignment. Transport. Sci. 11, 253–274.
Damberg, O., Lundgren, J.T., Patriksson, M., 1996. An algorithm for the stochastic user equilibrium problem. Transport. Res. Part B Methodol. 30 (2), 115–131.
Delafontaine, M., Versichele, M., Neutens, T., Van de Weghe, N., 2012. Analysing spatiotemporal sequences in Bluetooth tracking data. Appl. Geogr. 34, 659–668.
Di, X., Liu, H.X., Pang, J.S., Ban, X.J., 2013. Boundedly rational user equilibria (BRUE): mathematical formulation and solution sets. Proc. Soc. Behav. Sci. 80, 231–248.
Di, X., Liu, H.X., Ban, X.J., 2016. Second best toll pricing within the framework of bounded rationality. Transport. Res. Part B Methodol. 83, 74–90.
Dijkstra, E.W., 1959. A note on two problems in connexion with graphs. Numer. Math. (Heidelb) 1 (1), 269–271.
Duncan, L., Watling, D., Connors, R., Rasmussen, T.K., Nielsen, O.A., 2020. Path Size Logit Route Choice Models: Issues with Current Models, a New Internally Consistent Approach, and Parameter Estimation on a Large-Scale Network with GPS Data. Transport. Res. Part B Methodol. 135, 1–40.
Duncan, L., Watling, D., Connors, R., Rasmussen, T., Nielsen, O.A., 2022a. A bounded path size route choice model excluding unrealistic routes: formulation and estimation from a large-scale GPS study. Transportmetr. A Transport Sci. 18 (3), 435–493.
Duncan, L., Watling, D., Connors, R., Rasmussen, T., Nielsen, O.A., 2022b. Choice set robustness and internal consistency in correlation-based logit stochastic user equilibrium models. Transportmetr. A: Transport Sci. 19 (3), 2063969.
Duncan, L.C., Watling, D.P., Connors, R.D., Rasmussen, T.K., Nielsen, O.A., 2023. Formulation and solution method of bounded path size stochastic user equilibrium models–consistently addressing route overlap and unrealistic routes. Transportmetr. A: Transport Sci. 1–53.
Ehrgott, M., Wang, J.Y.T., Watling, D.P., 2015. On multi-objective stochastic user equilibrium. Transport. Res. Part B Methodol. 81, 704–717.
Friedrich, M., Hofsaess, I., Wekeck, S., 2001. Timetable-based transit assignment using branch and bound techniques. Transp. Res. Rec. 1752 (1), 100–107.
Friesz, T.L., Han, K., 2019. The mathematical foundations of dynamic user equilibrium. Transport. Res. Part B Methodol. 126, 309–328.
Gilbride, T.J., Allenby, G.M., 2004. A choice model with conjunctive, disjunctive, and compensatory screening rules. Market. Sci. 23 (3), 391–406.
Google,n.d.. [Google Maps directions to drive from Copenhagen, Denmark to Rome, Italy]. Retrieved June 08, 2023.
Guo, X., Liu, H.X., 2011. Bounded rationality and irreversible network change. Transport. Res. Part B Methodol. 45 (10), 1606–1618.
Hadjidimitriou, S.N., Dell'Amico, M., Cantelmo, G., Viti, F., 2015. Assessing the consistency between observed and modelled route choices through GPS data. In: Proceedings of the 2015 International Conference on Models and Technologies for Intelligent Transportation Systems (MT-ITS). Budapest, Hungary, pp. 216–222.
Han, S., 2003. Dynamic traffic modelling and dynamic stochastic user equilibrium assignment for general road networks. Transport. Res. Part B Methodol. 37 (3), 225–249.
Huang, K., Chen, M., Zhou, Z., Han, X., Wang, J., Liu, Z., 2023. A systematic approach for the calibration of route choice models based on stochastic user equilibrium. IEEE Intell. Transport. Syst. Magazine.
Huang, Z., Huang, Z., Zheng, P., Xu, W., 2018. Calibration of C-logit-based SUE route choice model using mobile phone data. Information 9 (5), 115.
Jedidi, K., Kohli, R., 2005. Probabilistic subset-conjunctive models for heterogeneous consumers. J. Market. Res. 42 (4), 483–494.
Jensen, A.F., Thorhauge, M., de Jong, G., Rich, J., Dekker, T., Johnson, D., Cabralb, M.O., Bates, J., Nielsen, O.A., 2019. A disaggregate freight transport chain choice model for Europe. Transport. Res. Part E Log. Transport. Rev. 121, 43–62.
Kim, T, Zhou, X., Pendyala, R.M., 2022. Computational graph-based framework for integrating econometric models and machine learning algorithms in emerging data-driven analytical environments. Transportmetrica A Transport. Sci. 18 (3), 1346–1375.
Kitthamkesorn, S., Chen, A., 2013. A path-size weibit stochastic user equilibrium model. Proc. Soc. Behav. Sci. 80, 608–632.
Kohli, R., Jedidi, K., 2005. Probabilistic subset conjunction. Psychometrika 70, 737–757.
Leong, W., Hensher, D.A., 2015. Contrasts of relative advantage maximisation with random utility maximisation and regret minimisation. *J. Transport Econ. Policy* (JTEP) 49 (1), 167–186.
Liu, H.X., He, X., He, B., 2009. Method of successive weighted averages (MSWA) and self regulated averaging schemes for solving stochastic user equilibrium problem. Netw. Spat. Econ. 9 (4), 485–503.
Liu, Z., Yin, Y., Bai, F., Grimm, D.K., 2023. End-to-end learning of user equilibrium with implicit neural networks. Transport. Res. Part C Emerg. Technol. 150, 104085.
Lou, Y., Yin, Y., Lawphongpanich, S., 2010. Robust congestion pricing under boundedly rational user equilibrium. Transport. Res. Part B Methodol. 44 (1), 15–28.
Luce, R., 1959. Individual choice behavior: a theoretical analysis. J. Wiley and Sons, New York.
Łukawska, M., Paulsen, M., Rasmussen, T.K., Jensen, A.F., Nielsen, O.A., 2023. A joint bicycle route choice model for various cycling frequencies and trip distances based on a large crowdsourced GPS dataset. Transport. Res. Part A Policy Pract. 176, 103834.
Mahmassani, H., Chang, G., 1987. On boundedly rational user equilibrium in transportation systems. Transport. Sci. 21 (2), 89–99.
Meng, Q., Lam, W.H., Yang, L., 2008. General stochastic user equilibrium traffic assignment problem with link capacity constraints. J. Adv. Transp. 42 (4), 429–465.
Mirzahossein, H., Gholampour, I., Sedghi, M., Zhu, L., 2021. How realistic is static traffic assignment? Analyzing automatic number-plate recognition data and image processing of real-time traffic maps for investigation. Transp. Res. Interdiscip. Perspect. 9, 100320.
Mohammadpour, S., Frejinger, E., 2022. Arc travel time and path choice model estimation subsumed. ArXiv. 2210.14351.
Nielsen, O.A., 1996. Do Stochastic traffic assignment models consider differences in road users' utility functions? Transportation planning methods. In: Proceedings of seminar E held at the PTRC European Transport Forum. Brunel University, U.K., p. 404. -2.
Nielsen, O.A., 2004. Behavioural responses to pricing schemes: Description of the Danish AKTA experiment. J. Intell. Transp. Syst. 8 (4), 233–251.
Prashker, J.N., Bekhor, S., 2004. Route choice models used in the stochastic user equilibrium problem: a review. Transp. Rev. 24 (4), 437–463.
Prato, C.G., Bekhor, S., 2006. Applying branch-and-bound technique to route choice set generation. Transp. Res. Rec. 1985 (1), 19–28.
Prato, C.G., Rasmussen, T.K., Nielsen, O.A., 2014. Estimating value of congestion and value of reliability from the observation of route choice behavior of car drivers. Transp. Res. Rec. 2412, 20–27. Transportation Research Board of the National Academies.
Prato, C.G., Halldórsdóttir, K., Nielsen, O.A., 2018. Evaluation of land-use and transport network effects on cyclists' route choices in the Copenhagen Region in value-of-distance space. Int. J. Sustain. Transp. 12 (10), 770–781.
Sheffi, Y., Powell, W.B., 1982. An algorithm for the equilibrium assignment problem with random link times. Networks 12, 191–207.
Shin, J., Ferguson, S., 2017. Exploring product solution differences due to choice model selection in the presence of noncompensatory decisions with conjunctive screening rules. J. Mech. Des. 139 (2), 021402.
Siripirote, T., Sumalee, A., Watling, D.P., Shao, H., 2014. Updating of Travel Behavior Model Parameters and Estimation of Vehicle Trip Chain Based on Plate Scanning. J. Intell. Transp. Syst. 18 (4), 393–409.
Smith, M.J., 1993. A new dynamic traffic model and the existence and calculation of dynamic user equilibria on congested capacity-constrained road networks. Transport. Res. Part B Methodol. 27 (1), 49–63.
Smith, M.J., Wisten, M.B., 1995. A continuous day-to-day traffic assignment model and the existence of a continuous dynamic user equilibrium. Ann. Oper. Res. 60.
Swait, J., 2001. A non-compensatory choice model incorporating attribute cutoffs. Transport. Res. Part B Methodol. 35 (10), 903–928.
Tversky, A., 1972. Elimination by aspects: A theory of choice. Psychol. Rev. 79 (4), 281–299.

Vovsha, P., 1997. Application of cross-nested logit model to mode choice in Tel Aviv, Israel, metropolitan area. Transp. Res. Rec. 1607, 6–15.
Wardrop, J., 1952. Some theoretical aspects of road traffic research. Proc. Inst. Civil Eng. Part II 1, 325–378.
Watling, D.P., Rasmussen, T.K., Prato, C.G., Nielsen, O.A., 2015. Stochastic user equilibrium with equilibrated choice sets: Part I–Model formulations under alternative distributions and restrictions. Transport. Res. Part B Methodol. 77, 166–181.
Watling, D., Rasmussen, T.K., Prato, C.G., Nielsen, O.A., 2018. Stochastic user equilibrium with a bounded choice model. Transport. Res. Part B Methodol. 114, 254–280.
Wei, C., Asakura, Y., 2013. A Bayesian approach to traffic estimation in stochastic user equilibrium networks. Transport. Res. Part C Emerg. Technol. 36, 446–459.
Zhang, J., Timmermans, H., Borgers, A., Wang, D., 2004. Modeling traveler choice behavior using the concepts of relative utility and relative interest. Transport. Res. Part B Methodol. 38 (3), 215–234.
Zhang, J., 2013. A generalized relative utility based choice model with multiple context dependencies. In: Proceedings of the International Choice Modelling Conference, pp. 3–5.
Zhang, J., 2015. Relative utility modelling. Bounded rational choice behaviour: Applications in transport. Emerald Group Publishing Limited, pp. 49–71.
Zhou, Z., Chen, A., Bekhor, S., 2012. C-logit stochastic user equilibrium model: formulations and solution algorithm. Transportmetrica 8 (1), 17–41.
Zhu, S., Levinson, D., 2015. Do people use the shortest path? An empirical test of Wardrop's first principle. PLoS. ONE 10 (8), e0134322.